Available online at www.sciencedirect.com

ScienceDirect

Nuclear Physics B 946 (2019) 114718

NUCLEAR PHYSICS B

www.elsevier.com/locate/nuclphysb

A study of $\Delta C = 1$ decays of bottom mesons involving axial-vector meson

Neelesh Sharma [a], Rohit Dhir [b,*]

[a] *SRM Research Institute, SRM Institute of Science and Technology, Kattankulathur 603203, India*

[b] *Department of Physics and Nanotechnology, SRM Institute of Science and Technology, Kattankulathur 603203, India*

Received 23 August 2018; received in revised form 4 July 2019; accepted 22 July 2019

Available online 30 July 2019

Editor: Hong-Jian He

Abstract

We study the two-body charmed nonleptonic weak decays of the bottom meson to an axial-vector meson and a pseudoscalar meson using the non-relativistic quark model. We employ the factorization hypothesis to obtain the branching ratios of these decays. First, we calculate the axial-vector ($J^P = 1^+$) emitting form factors for $B \to D_1/\underline{D}_1$ transitions in the non-relativistic Isgur-Scora-Grinstein-Wise quark model. Later, we use the heavy quark symmetry constraints to obtain the $B \to D_1^{1/2}/D_1^{3/2}$ form factors and consequently, calculated their branching ratios. For a comparative analysis, we extract $\tau_{1/2}(\omega)$ and $\tau_{3/2}(\omega)$ form factors from the recent lattice QCD results to get a qualitative estimate of $B \to D_1^{1/2}/D_1^{3/2}$ form factors. We find that the calculated branching ratios are in fair agreement with the available experimental data in both the scenarios. Also, we observe that, despite of $1/m_Q$ suppression in heavy quark limit, the color-suppressed contribution to these decays can not be ignored.

1. Introduction

The phenomenological analyses of the bottom (B) meson decays provide exciting opportunities to test several models and the approaches within and beyond the Standard Model (SM). The

* Corresponding author.

E-mail addresses: nishu.vats@gmail.com (N. Sharma), dhir.rohit@gmail.com (R. Dhir).

https://doi.org/10.1016/j.nuclphysb.2019.114718

0550-3213/

understanding of B physics serves as a tool to study the interplay of strong and weak interaction dynamics in the SM and also a test of the new physics beyond the SM. The time to time comparison between the theoretical predictions and the experimental results help in better understanding of the hadronic structure in heavy bound states. In heavy flavor hadrons, the theoretical interpretation of the nonleptonic decays are still under progress for being non-perturbative in nature. The factorization hypothesis has been successfully used to study such decays as it suits the description of B decaying to heavy mesons [1–8]. Also, the mass of b-quark is much heavier than the quantum chromodynamics (QCD) scale, where the dynamics becomes much simpler in the light of heavy quark symmetries [3,4,7]. The heavy quark symmetry (HQS) proves to be a very useful tool to provide symmetry relations for the heavy meson decays, however, one still has to use some model to obtain the explicit expressions for the decay rates. There are several models *like* Bauer, Stech & Wirbel (BSW) [3,4], Isgur-Scora-Grinstein-Wise (ISGW) [5,6], and covariant light front (CLF) [9] which can efficaciously be used in the light of heavy quark effective theory (HQET). Unlike the present study, in heavy to light decays the final state mesons have large energy, where the approaches *like* light cone sum rules (LCSR), soft collinear effective theory (SCET), and perturbative QCD have worked reasonably well to understand the experimental data [7,8]. Several theoretical frameworks based on the factorization hypothesis, relativistic quark model, HQET, CLF approach, perturbative QCD, *etc*. has been employed to study the *charmless* axial-vector meson emitting decays of B mesons [9–16]. It is worth remarking here that the dominant modes in the charmed sector of these decays proceed mainly through the tree level diagrams and thus, are least influenced by the penguin pollution. Hence, the *charmed* p-wave meson emitting decays are considered using the factorization scheme and HQS in the non-relativistic quark models, CLF approach, SCET, perturbative QCD based modeling, HQET, and Bakamjian-Thomas (BT) relativistic quark model [16–30]. In recent past, several attempts have been made to determine the form factors of $B \to D^{**}$ transitions in heavy quark limit [28–38]. The importance of theoretical uncertainties arising from the $\Lambda_{\rm QCD}/m_Q$ corrections, in all the form factors for heavy quark expansion, has been emphasized. Since, in the heavy quark limit some form factors could be suppressed at zero recoil, therefore such corrections could be decisive. Most recently, it is pointed out that the contributions from the corrections of $\mathcal{O}(\Lambda_{\rm QCD}/m_Q)$ to the new physics matrix elements could be dominant [39].

On the experimental side, recent observations, *especially*, of many strange charm resonances, and many proposed experiments (see for review [40]) has revived the interests of hadronic physicists to study the orbitally excited mesons. In the weak decay sector, the branching ratios of many of the decay modes involving charm meson in the final state e.g. $B^- \to D^0 a_1^-$, $B^- \to \pi^- \underline{D}_1^0$, $B^- \to \pi^- \chi_{c1}$, $\bar{B}^0 \to D^+ a_1^-$, $\bar{B}^0 \to \chi_{c1}\pi^0$, $\bar{B}^0 \to \bar{K}^0 \chi_{c1}$ *etc.* [41] have been measured to be $\mathcal{O}(10^{-3}) \sim \mathcal{O}(10^{-5})$ (as shown in Table 1). Therefore, we will focus our study to analyze the $B \to PA$ decay modes involving charmed meson in the final state.

In this work, we have investigated the axial-vector meson emitting decays of B meson involving charmed mesons in the Cabibbo-Kobayashi-Maskawa (CKM) allowed and suppressed modes. In ***scenario-I***, we employ the improved version of ISGW [6] quark model, to evaluate the $B \to A/A'$ transition form factors. It is worth mentioning that the ISGW II incorporates heavy quark symmetry constraints and hyperfine distortions of the wave functions. For a long time, beside the recent CLF model, ISGW II quark model has been the only model to give the reliable transition form factors from the ground state s-wave mesons to a low-lying p-wave mesons. For $B \to P$ transition form factors, we rely upon the lattice QCD results, which are also consistent with the LCSR calculations [42–45]. Using the factorization scheme, we calculated the branching ratios of these decay modes. We found that the calculated branching ratios of the

Table 1
Experimentally measured branching ratios for $B \to PA$ decays.

Mode	Experimental Branchings [41]
$B^- \to D^0 a_1^-$	$(4 \pm 4) \times 10^{-3}$
$B^- \to \pi^- \underline{D}_1^0$	$(1.5 \pm 0.6) \times 10^{-3}$
$B^- \to \pi^- D_1^0$	$(7.5 \pm 1.7) \times 10^{-4}$[19]
$B^- \to \pi^- \chi_{c1}$	$(2.2 \pm 0.5) \times 10^{-5}$
$B^- \to K^- \chi_{c1}$	$(4.79 \pm 0.23) \times 10^{-4}$
$B^- \to \bar{K}^0 a_1^-$	$(3.5 \pm 0.7) \times 10^{-5}$
$B^- \to \pi^0 a_1^-$	$(2.6 \pm 0.7) \times 10^{-5}$
$B^- \to \pi^- a_1^0$	$(2.0 \pm 0.6) \times 10^{-5}$
$\bar{B}^0 \to D^+ a_1^-$	$(6.0 \pm 3.3) \times 10^{-3}$
$\bar{B}^0 \to \chi_{c1} \pi^0$	$(1.12 \pm 0.28) \times 10^{-5}$
$\bar{B}^0 \to \bar{K}^0 \chi_{c1}$	$(3.9 \pm 0.4) \times 10^{-4}$
$\bar{B}^0 \to K^- a_1^+$	$(1.6 \pm 0.4) \times 10^{-5}$
$\bar{B}^0 \to \pi^\mp a_1^\pm$	$(2.6 \pm 0.5) \times 10^{-5}$
$B^- \to D_s^- a_1^0$	$< 1.8 \times 10^{-3}$
$B^- \to \pi^- \bar{K}_1^0(1270)$	$< 4.0 \times 10^{-5}$
$B^- \to \pi^- \bar{K}_1^0(1400)$	$< 3.9 \times 10^{-5}$
$\bar{B}^0 \to D_s^- a_1^+$	$< 2.1 \times 10^{-3}$
$\bar{B}^0 \to \pi^+ K_1^-(1270)$	$< 3.0 \times 10^{-5}$
$\bar{B}^0 \to \pi^+ K_1^-(1400)$	$< 2.7 \times 10^{-5}$
$\bar{B}^0 \to \pi^0 a_1^0$.	$< 1.1 \times 10^{-3}$

Cabibbo-favored modes such as, $B^- \to D^0 a_1^-$, $B^- \to \pi^- \underline{D}_1^0$, and $B^- \to \pi^- D_1^0$ are in very good agreement with the experimental numbers.

Another, aim of the present analysis is to discuss the effects of heavy quark symmetry on axial-vector meson emitting decays involving D_1 and D_{s1} mesons. Based on the HQS analyses, the importance of color-suppressed contributions has been pointed out in the past [19,21]. It has been indicated that the larger magnitude of the color-suppressed contributions is necessary to explain the existing experimental data. Therefore, in ***scenario-II***, we extend our calculation to obtain the $B \to D_{1/2}/D_{3/2}$ transition form factors in the ISGW II model within HQS constraints. In addition to this, we use the lattice QCD results for the Isgur-Wise form factors, $\tau_{1/2}(1)$ and $\tau_{3/2}(1)$, at zero recoil to extract a crude guess of $B \to D_{1/2}/D_{3/2}$ form factors, phenomenologically. It is interesting to note that the calculated form factors are in reasonably good agreement with the $\tau_{1/2}(\omega)$ and $\tau_{3/2}(\omega)$ extracted from the experimental data. We understand that the $1/m_Q$ corrections could be essential but at the same time the lattice QCD results could be trusted for their systematic approach to QCD. We found that the calculated branching ratios in HQS, for both ISGW II and lattice QCD inspired calculations, compared well with the existing theoretical and experimental results. Comparison with the experimental observations reveal that the magnitude (as well as the sign) of the color-suppressed contributions in these decays could be larger than the theoretical estimates. Also, we find some of these decay channels, especially involving D_{s1} states, have large branching ratios *i.e.* comparable to that of the *s*-wave mesons emitting decay modes and are well within the reach of future experiments.

The paper is organized as follows. In sec. 2, the meson spectroscopy is discussed. Methodology for the framework is presented in sec. 3. In sec. 4, we discuss the decay constants and form factors in the light of heavy quark symmetry constraints. Numerical results and discussions are presented in the sec. 5 and the summary and conclusions are given in the last section.

2. Meson spectroscopy

The both types of axial-vector mesons, ${}^3P_1$ ($J^{PC} = 1^{++}$) and ${}^1P_1$ ($J^{PC} = 1^{+-}$), behave well with respect to the quark model $q\bar{q}$ assignments. Strange and charmed states are most likely a mixture of ${}^3P_1$ and ${}^1P_1$ states, since there is no quantum number forbidding such mixing. In contrast, diagonal ${}^3P_1$ and ${}^1P_1$ systems have opposite C-parity and cannot mix. Experimentally [41], the following non-strange and uncharmed mesons have been observed:

i. for ${}^3P_1$ multiplet, isovector $a_1(1.230)$ and two isoscalars $f_1(1.282)$ and $f_1'(1.426)$;
ii. for ${}^1P_1$ multiplet, isovector $b_1(1.229)$ and two isoscalars $h_1(1.170)$ and $h_1'(1.386)$. C-parity of $h_1'(1.386)$ and spin and parity of the $h_{c1}(3.526)$ remains to be confirmed.

Numerical values given in the bracket indicates mass (in GeV) of the respective mesons. In the present analysis, mixing of the isoscalar states of (1^{++}) mesons is defined as

$$\begin{aligned} f_1(1.282) &= \frac{1}{\sqrt{2}}(u\overline{u} + d\overline{d})\cos\phi_A + (s\overline{s})\sin\phi_A, \\ f_1'(1.426) &= \frac{1}{\sqrt{2}}(u\overline{u} + d\overline{d})\sin\phi_A - (s\overline{s})\cos\phi_A, \\ \chi_{c1}(3.511) &= (c\bar{c}), \end{aligned} \tag{1}$$

where

$$\phi_A = \theta(ideal) - \theta_A(physical).$$

Similarly, mixing of the two isoscalar mesons $h_1(1.170)$ and $h\prime_1(1.386)$ is defined as:

$$\begin{aligned} h_1(1.170) &= \frac{1}{\sqrt{2}}(u\overline{u} + d\overline{d})\cos\phi_{A'} + (s\overline{s})\sin\phi_{A'}, \\ h_1'(1.386) &= \frac{1}{\sqrt{2}}(u\overline{u} + d\overline{d})\sin\phi_{A'} - (s\overline{s})\cos\phi_{A'}, \\ h_{c1}(3.526) &= (c\bar{c}). \end{aligned} \tag{2}$$

Proximity of $a_1(1.230)$ and $f_1(1.282)$ and, to lesser extent, that of $b_1(1.229)$ and $h_1(1.170)$ indicates the ideal mixing for both 1^{++} and 1^{+-} nonets, supported by their decay patterns i.e.,

$$\phi_A = \phi_{A'} = 0^\circ. \tag{3}$$

States involving a strange quark of $A(J^{PC} = 1^{++})$ and $A'(J^{PC} = 1^{+-})$ mesons mix to generate the physical states in the following manner:

$$\begin{aligned} K_1(1.270) &= K_{1A}\sin\theta_1 + K_{1A'}\cos\theta_1, \\ \underline{K}_1(1.400) &= K_{1A}\cos\theta_1 - K_{1A'}\sin\theta_1, \end{aligned} \tag{4}$$

where K_{1A} and $K_{1A'}$ are the strange partners of $a_1(1.230)$ and $b_1(1.229)$, respectively. Particle Data Group [41] assumes that the mixing is maximal, i.e., $\theta_1 = 45^\circ$, whereas $\tau \to K_1(1.270)/K_1(1.400) + \nu_\tau$ data yields $\theta_1 = \pm 37^\circ$ and $\theta_1 = \pm 58^\circ$ [9,18,19]. Furthermore, the study of $D \to K_1(1.270)\pi$, $K_1(1.400)\pi$ decay rules out positive mixing-angle solutions and $\theta_1 = -58^\circ$ [9] is experimentally favored. However, in a recent phenomenological analysis [46], it has been shown that the choice of angles for $f - f'$ and $h - h'$ mixing schemes (that favors ideal mixing) are closely related to the choice of the mixing angle θ_1, therefore, a mixing angle $\sim 35^\circ$ is preferred over $\sim 55^\circ$. Hence, we use $\theta_1 = -37^\circ$ in our numerical calculations.

The mixing of charmed and strange-charmed state mesons are given in a similar fashion,

$$\begin{aligned} D_1(2.427) &= D_{1A}\sin\theta_{D_1} + D_{1A'}\cos\theta_{D_1}, \\ \underline{D}_1(2.422) &= D_{1A}\cos\theta_{D_1} - D_{1A'}\sin\theta_{D_1}, \end{aligned} \tag{5}$$

and

$$\begin{aligned} D_{s1}(2.460) &= D_{s1A}\sin\theta_{D_{s1}} + D_{s1A'}\cos\theta_{D_{s1}}, \\ \underline{D}_{s1}(2.535) &= D_{s1A}\cos\theta_{D_{s1}} - D_{s1A'}\sin\theta_{D_{s1}}. \end{aligned} \tag{6}$$

However, in the heavy quark limit, the physical mass eigenstates with $J^P = 1^+$ are $P_1^{3/2}$ and $P_1^{1/2}$ rather than ${}^3P_1$ and ${}^1P_1$ states as the heavy quark spin S_Q decouples from the other degrees of freedom, so that S_Q and the total angular momentum of the light antiquark are separately a good quantum numbers [47]. Therefore, we can write

$$\begin{aligned} |P_1^{1/2}> &= \sqrt{\tfrac{1}{3}}|{}^1P_1> - \sqrt{\tfrac{2}{3}}|{}^3P_1>, \\ |P_1^{3/2}> &= \sqrt{\tfrac{2}{3}}|{}^1P_1> + \sqrt{\tfrac{1}{3}}|{}^3P_1>. \end{aligned} \tag{7}$$

Hence, the states $D_1(2.427)$ and $\underline{D}_1(2.422)$ can be identified with $P_1^{1/2}$ and $P_1^{3/2}$, respectively. However, beyond the heavy quark limit, there is a mixing between $P_1^{1/2}$ and $P_1^{3/2}$ denoted by

$$\begin{aligned} D_1(2.427) &= D_1^{1/2}\cos\theta_2 + D_1^{3/2}\sin\theta_2, \\ \underline{D}_1(2.422) &= -D_1^{1/2}\sin\theta_2 + D_1^{3/2}\cos\theta_2. \end{aligned} \tag{8}$$

The mixing angle $\theta_2 = (-5.7 \pm 2.4)^\circ$ is obtained by the Belle through a detailed analysis [48]. However, we use a positive mixing angle $\theta_{D_1} = 17^\circ$ based on the study of $D_1(2427)\pi$ production in B decays [18]. Likewise for the strange axial-vector charmed mesons,

$$\begin{aligned} D_{s1}(2.460) &= D_{s1}^{1/2}\cos\theta_3 + D_{s1}^{3/2}\sin\theta_3, \\ \underline{D}_{s1}(2.535) &= -D_{s1}^{1/2}\sin\theta_3 + D_{s1}^{3/2}\cos\theta_3. \end{aligned} \tag{9}$$

$\theta_3 \approx 7^\circ$ is determined from the quark potential model [18,19,49]. For η and η' pseudoscalar states, we use

$$\begin{aligned} \eta(0.547) &= \tfrac{1}{\sqrt{2}}(u\overline{u} + d\overline{d})\sin\phi_P - (s\overline{s})\cos\phi_P, \\ \eta'(0.958) &= \tfrac{1}{\sqrt{2}}(u\overline{u} + d\overline{d})\cos\phi_P + (s\overline{s})\sin\phi_P, \end{aligned} \tag{10}$$

where $\phi_P = \theta_{ideal} - \theta_{physical}$, $\theta_{physical} = -15.4^\circ$. η_c is taken as $\eta_c(2.979) = (c\bar{c})$.

3. Methodology

3.1. Weak Hamiltonian

For the bottom changing $\Delta b = 1$ decays, the weak Hamiltonian involves the bottom changing current,

$$J_\mu = (\bar{c}b)V_{cb} + (\bar{u}b)V_{ub}, \tag{11}$$

where $(\bar{q}_i q_j) \equiv \bar{q}_i \gamma_\mu (1-\gamma_5) q_j$ denotes the weak *V-A* current. QCD modified weak Hamiltonian is then given below:

a. for decays involving $b \to c$ transition,

$$H_W = \frac{G_F}{\sqrt{2}} \big\{ V_{cb} V_{ud}^* [a_1 (\bar{c}b)(\bar{d}u) + a_2 (\bar{d}b)(\bar{c}u)] + V_{cb} V_{cs}^* [a_1 (\bar{c}b)(\bar{s}c) + a_2 (\bar{s}b)(\bar{c}c)] \\ + V_{cb} V_{us}^* [a_1 (\bar{c}b)(\bar{s}u) + a_2 (\bar{s}b)(\bar{c}u)] + V_{cb} V_{cd}^* [a_1 (\bar{c}b)(\bar{d}c) + a_2 (\bar{d}b)(\bar{c}c)] \big\}, \quad (12)$$

b. for decays involving $b \to u$ transition,

$$H_W = \frac{G_F}{\sqrt{2}} \big\{ V_{ub} V_{cs}^* [a_1 (\bar{u}b)(\bar{s}c) + a_2 (\bar{s}b)(\bar{u}c)] + V_{ub} V_{ud}^* [a_1 (\bar{u}b)(\bar{d}u) + a_2 (\bar{d}b)(\bar{u}u)] \\ + V_{ub} V_{us}^* [a_1 (\bar{u}b)(\bar{s}u) + a_2 (\bar{s}b)(\bar{u}u)] + V_{ub} V_{cd}^* [a_1 (\bar{u}b)(\bar{d}c) + a_2 (\bar{d}b)(\bar{u}c)] \big\}. \quad (13)$$

By factorizing matrix elements of the four-quark operator contained in the effective Hamiltonian (12) and (13), one can distinguish three classes of decays [3,4]:

1. The first class (Class I) contains those decays which can be generated from the color singlet current; and the decay amplitudes are proportional to a_1, where $a_1(\mu) = c_1(\mu) + \frac{1}{N_c} c_2(\mu)$, and N_c is the number of colors.
2. The second class (Class II) of transition consists those decays which can be generated from the neutral current. The decay amplitude in this class is proportional to a_2 *i.e.* for the color-suppressed modes, $a_2(\mu) = c_2(\mu) + \frac{1}{N_c} c_1(\mu)$.
3. The third class (Class III) of decay modes can be generated from the interference of color singlet and color neutral currents *i.e.* the a_1 and a_2 amplitudes interfere.

Hence, we use $N_c = 3$ to fix the effective QCD coefficients:

$$a_1 = 1.03 \text{ and } a_2 = 0.11, \quad (14)$$

where $c_1(\mu) = 1.12$, and $c_2(\mu) = -0.26$ at $\mu \approx m_b^2$ [4,7].

It may be noted that the decay amplitudes can be expressed as a factorizable contribution multiplied by the corresponding a_i's that are (renormalization) scale dependent, however are expected to be process independent. In addition to the $1/N_c$ terms in naive factorization, the a_1 and a_2 evaluated at sub-leading orders in $1/N_c$ receive contributions from the nonfactorizable effects that are non-perturbative in nature [50–52]. Analyses of $B \to D\pi$ shows that the ratio of effective a_1 and a_2 *i.e.* a_1^{eff} and a_2^{eff} to confront the experimental measurements for $B \to D\pi$ data is expected to be $|a_2^{eff}/a_1^{eff}| \sim (0.45 - 0.65)e^{\pm i60}$ [53]. Furthermore, a_2 parameter cannot be calculated in the QCD factorization for $\bar{B} \to D^{**}\pi$ type decays because D meson being heavy and slow cannot be decoupled from $(B\pi)$ system. Thus, soft interaction between $(B\pi)$ system and the charm quark of D meson will be considerably different from the interaction between the $(B\pi)$ system and light spectator quark of D meson [54].

As we have mentioned earlier, B decays either only via tree diagrams or are tree dominated, therefore we neglect the expected small penguin contributions in our formalism.

3.2. Decay rates

The decay rate formula for $B \to PA$ decay is given by

$$\Gamma(B \to PA) = \frac{p_c^3}{8\pi m_A^2} |A(B \to PA)|^2 , \tag{15}$$

where p_c is the magnitude of the three-momentum of a final-state particle in the rest frame of B meson and m_A denotes the mass of the axial-vector meson.

The factorization scheme express the decay amplitudes as a product of the matrix elements of weak currents (up to the weak scale factor of $\frac{G_F}{\sqrt{2}} \times$ CKM elements $\times$ QCD factor) as

$$\langle PA| H_w |B\rangle \approx \langle P| J^\mu |0\rangle \langle A| J_\mu |B\rangle + \langle A| J^\mu |0\rangle \langle P| J_\mu |B\rangle , \tag{16}$$

$$\left\langle PA'\right| H_w |B\rangle \approx \langle P| J^\mu |0\rangle \left\langle A'\right| J_\mu |B\rangle + \left\langle A'\right| J^\mu |0\rangle \langle P| J_\mu |B\rangle . \tag{17}$$

Using the Lorentz invariance, matrix elements of the current between meson states can be expressed [6] as

$$\langle P| J_\mu |0\rangle = -i f_P k_\mu , \tag{18}$$

$$\langle A| J_\mu |0\rangle = \varepsilon^*_\mu m_A f_A , \tag{19}$$

$$\left\langle A'\right| J_\mu |0\rangle = \varepsilon^*_\mu m_{A'} f_{A'} , \tag{20}$$

$$\langle A(P_A)|J_\mu|B(P_B)\rangle = \ell \varepsilon^*_\mu + c_+(\varepsilon^* \cdot P_B)(P_B + P_A)_\mu + c_-(\varepsilon^* \cdot P_B)(P_B - P_A)_\mu , \tag{21}$$

$$\left\langle A'(P_{A'})\right|J_\mu|B(P_B)\rangle = r \varepsilon^*_\mu + s_+(\varepsilon^* \cdot P_B)(P_B + P_{A'})_\mu + s_-(\varepsilon^* \cdot P_B)(P_B - P_{A'})_\mu , \tag{22}$$

and

$$\langle P(P_P)| J_\mu |B(P_B)\rangle = (P_{B\mu} + P_{P\mu} - \frac{m_B^2 - m_P^2}{q^2} q_\mu) F_1^{BP}(q^2) + \frac{m_B^2 - m_P^2}{q^2} q_\mu F_0^{BP}(q^2). \tag{23}$$

4. Decay constants and form factors

4.1. Decay constants

In this work, we are using the following values of the decay constants [38,41,55] for pseudoscalar mesons (0^-) those are well known:

$$f_\pi = 0.131 \text{ GeV}, \; f_K = 0.160 \text{ GeV},$$
$$f_D = 0.212 \text{ GeV}, \; f_{D_s} = 0.249 \text{ GeV},$$
$$f_\eta = 0.133 \text{ GeV}, \; f_{\eta'} = 0.126 \text{ GeV}, \text{ and } f_{\eta_c} = 0.400 \text{ GeV}.$$

However, for axial-vector mesons (1^+), the decay constants for $J^{PC} = 1^{+-}$ mesons may vanish due to the C-parity behavior. Under charge conjunction, the two types of axial-vector mesons transform as

$$\begin{aligned} M_b^a(1^{++}) &\to +M_a^b(1^{++}) \\ M_b^a(1^{+-}) &\to -M_a^b(1^{+-}) \end{aligned} \tag{24}$$

where $(a, b = 1, 2, 3)$ and M^a_b denotes meson 3×3 matrix elements in SU(3) flavor symmetry. Since the weak axial-vector current transforms as $(A_\mu)^a_b \to +(A_\mu)^b_a$ under charge conjunction, only the (1^{++}) state can be produced through the axial-vector current in the SU(3) symmetry limit [56,57]. Particle Data Group [41] assumes that the mixing is maximal, i.e., $\theta = 45^0$, whereas $\tau \to K_1(1.270)/K_1(1.400) + \nu_\tau$ data yields $\theta = \pm 37^0$ and $\theta = \pm 58^0$.

To determine the decay constant of $K_1(1.270)$, we use the following formula:

$$\Gamma(\tau \to K_1\nu_\tau) = \frac{G_F^2}{16\pi}|V_{us}|^2 f_{K_1}^2 \frac{(m_\tau^2 + 2m_{K_1}^2)(m_\tau^2 - m_{K_1}^2)^2}{m_\tau^3},$$

which gives $f_{K_1(1270)} = 0.175 \pm 0.019$ GeV. The decay constant of $K_1(1.400)$ can be obtained from $f_{K_1(1.400)} \big/ f_{K_1(1.270)} = \cot\theta$. A small value around 0.011 GeV for the decay constant of K_{1B} may arise through SU(3) breaking, which yields $f_{\underline{K}_1(1.400)} = f_{K_{1A}}\cos\theta_1 - f_{K_{1B}}\sin\theta_1 = -0.232$ GeV for $\theta_1 = -37°$ (-0.087 GeV for $\theta_1 = -58°$) [9]. Similarly, decay constant of $a_1(1.260)$ can be obtained from $B(\tau \to a_1\nu_\tau)$. However, this branching ratio is not given in the Particle Data Group [41], although the data on $\tau \to a_1\nu_\tau \to \rho\pi\nu_\tau$ have been reported by the various experiments. We take $f_{a_1} = 0.203 \pm 0.018$ GeV from the analysis given by J.C.R. Bloch et al. [58]. For the decay constant of $f_1(1.285)$, we assume $f_{f_1} \approx f_{a_1}$. The decay constants,

$$\begin{aligned}
&f_{D_{1A}} = -0.177 \text{ GeV}, \; f_{D_{1B}} = 0.060 \text{ GeV}, \\
&f_{D_{s1A}} = -0.160 \text{ GeV}, \; f_{D_{s1B}} = 0.042 \text{ GeV}, \text{ and } f_{\chi_{c1}} \approx -0.207 \text{ GeV}.
\end{aligned}$$

have been taken from [9,38].

4.2. The $B \to A/A'$ transition form factors in ISGW II quark model

We used the improved ISGW II quark model which describes a more realistic behavior of the form-factor at large momentum transfer *i.e.* $(q_m^2 - q^2)$. In addition to this, the ISGW II model includes various ingredients, such as the heavy quark symmetry constraints, the heavy quark symmetry breaking color-magnetic interaction, relativistic corrections, etc. The form factors have the following expressions [6].

$$\begin{aligned}
q &= -\frac{m_d}{2\tilde{m}_A\beta_B}\left(\frac{5+\tilde{\omega}}{6}\right)F_5^{(q)}, \\
\ell &= -\tilde{m}_B\beta_B\left[\frac{1}{\mu_-} + \frac{m_2\tilde{m}_A(\tilde{\omega}-1)}{\beta_B^2}\left(\frac{5+\tilde{\omega}}{6m_1} - \frac{m_2\beta_B^2}{2\mu_-\beta_{BA}^2}\right)\right]F_5^{(\ell)}, \\
c_+ + c_- &= -\frac{m_2\tilde{m}_A}{2m_1\tilde{m}_B\beta_B}\left(1 - \frac{m_1m_2\beta_B^2}{2\tilde{m}_A\mu_-\beta_{BA}^2}\right)F^{(c_+ + c_-)}, \\
c_+ - c_- &= -\frac{m_2\tilde{m}_A}{2m_1\tilde{m}_B\beta_B}\left(\frac{\tilde{\omega}+2}{3} - \frac{m_1m_2\beta_B^2}{2\tilde{m}_A\mu_-\beta_{BA}^2}\right)F^{(c_+ - c_-)}, \\
r &= \frac{\tilde{m}_B\beta_B}{\sqrt{2}}\left[\frac{1}{\mu_+} + \frac{m_2\tilde{m}_A}{3m_1\beta_B^2}(\tilde{\omega}-1)^2\right]F_5^{(r)}, \\
s_+ + s_- &= -\frac{m_2}{2\tilde{m}_B\beta_B}\left(1 - \frac{m_2}{m_1} + \frac{m_2\beta_B^2}{2\mu_+\beta_{BA}^2}\right)F^{(s_+ + s_-)}, \\
s_+ - s_- &= -\frac{m_2}{2m_1\beta_B}\left(\frac{4-\tilde{\omega}}{3} - \frac{m_1m_2\beta_B^2}{2\tilde{m}_A\mu_+\beta_{BA}^2}\right)F^{(s_+ - s_-)},
\end{aligned} \tag{25}$$

Table 2
The parameter β for s-wave and p-wave mesons in the ISGW II quark model.

Quark content	$u\bar{d}$	$u\bar{s}$	$s\bar{s}$	$c\bar{u}$	$c\bar{s}$	$u\bar{b}$	$s\bar{b}$	$c\bar{c}$
β_s(GeV)	0.41	0.44	0.53	0.45	0.56	0.43	0.54	0.88
β_p(GeV)	0.28	0.30	0.33	0.33	0.38	0.35	0.41	0.52

where

$$\begin{aligned} F_5^{(l)} &= F_5^{(r)} = F_5(\frac{\bar{m}_B}{\tilde{m}_B})^{1/2}(\frac{\bar{m}_A}{\tilde{m}_A})^{1/2}, \\ F_5^{(c_++c_-)} &= F_5^{(s_++s_-)} = F_5(\frac{\bar{m}_B}{\tilde{m}_B})^{-3/2}(\frac{\bar{m}_A}{\tilde{m}_A})^{1/2}, \\ F_5^{(c_+-c_-)} &= F_5^{(s_+-s_-)} = F_5(\frac{\bar{m}_B}{\tilde{m}_B})^{-1/2}(\frac{\bar{m}_A}{\tilde{m}_A})^{-1/2}. \end{aligned} \tag{26}$$

The $t\,(\equiv q^2)$dependence is given by

$$\tilde{\omega} - 1 = \frac{t_m - t}{2\bar{m}_B\bar{m}_A}, \tag{27}$$

and

$$F_5 = \left(\frac{\tilde{m}_A}{\tilde{m}_B}\right)^{1/2}\left(\frac{\beta_B\beta_A}{B_{BA}}\right)^{5/2}\left[1 + \frac{1}{18}h^2(t_m - t)\right]^{-3}, \tag{28}$$

where

$$h^2 = \frac{3}{4m_c m_q} + \frac{3m_d^2}{2\bar{m}_B\bar{m}_A\beta_{BA}^2} + \frac{1}{\bar{m}_B\bar{m}_A}(\frac{16}{33-2n_f})\ln[\frac{\alpha_S(\mu_{QM})}{\alpha_S(m_q)}],$$

with

$$\beta_{BA}^2 = \frac{1}{2}\left(\beta_B^2 + \beta_A^2\right), \tag{29}$$

and

$$\mu_\pm = \left(\frac{1}{m_q} \pm \frac{1}{m_b}\right)^{-1}.$$

$\tilde{m}$ is the sum of the mesons constituent quarks masses, $\bar{m}$ is the hyperfine averaged physical masses, n_f is the number of active flavors, $t_m = (m_B - m_A)^2$ is the maximum momentum transfer and μ_{QM} is the quark model scale. The subscript q depends upon the quark currents $\bar{q}\gamma_\mu b$ and $\bar{q}\gamma_\mu\gamma_5 b$ appearing in different transitions. The values of the parameter β for different s-wave and p-wave mesons are given in the Table 2. We use the following constituent quark masses (in GeV)

$$m_u = m_d = 0.31 \pm 0.04,\ m_s = 0.49 \pm 0.04,\ m_c = 1.7 \pm 0.04,\ \text{and}\ m_b = 5.0 \pm 0.04,$$

to calculate the form factors for $B \to A$ and $B \to A'$ transitions. The obtained form factors are given in Tables 3 and 4. It is worth noting that the calculated form factors are sensitive to the choice of quark masses. Therefore we allow the above given variation, particularly in light-quark sector, which may lead to uncertainties in the form factors.

Table 3
Form factors of $B(0^-) \to A(1^+)$ transition at $q^2 = m_\pi^2$ in the ISGW II quark model.

Transition	l	c_+	c_-
$B \to a_1$	$-2.01^{+0.17}_{-0.66}$	$-0.011^{+0.000}_{-0.001}$	$-0.0014^{+0.0005}_{-0.0007}$
$B \to f_1$	$-2.03^{+0.18}_{-0.66}$	$-0.011^{+0.0000}_{-0.001}$	-0.0015 ± 0.0005
$B \to K_1$	-1.77 ± 0.01	-0.013 ± 0.001	-0.0013 ± 0.0004
$B \to D_1$	-1.10 ± 0.05	-0.034 ± 0.004	$-0.0016^{+0.0004}_{-0.0001}$

Table 4
Form factors of $B(0^-) \to A'(1^+)$ transition at $q^2 = m_\pi^2$ in the ISGW II quark model.

Transition	r	s_+	s_-
$B \to b_1$	$1.10^{+0.40}_{-0.14}$	$0.017^{+0.002}_{-0.000}$	-0.007 ± 0.001
$B \to h_1$	$1.10^{+0.46}_{-0.15}$	$0.015^{+0.003}_{-0.000}$	$-0.006^{+0.000}_{-0.001}$
$B \to \underline{K}_1$	0.89 ± 0.04	0.025 ± 0.002	-0.011 ± 0.001
$B \to \underline{D}_1$	0.66 ± 0.02	0.068 ± 0.004	-0.023 ± 0.002

Table 5
Form factors of $B \to D_1^{1/2}, D_1^{3/2}$ transitions at $q^2 = m_\pi^2$ in the ISGW II quark model and LQCD estimates using $\tau_{1/2}(1) = 0.296$, $\tau_{3/2}(1) = 0.526$.

Transition	ℓ	c_+	c_-
ISGW II with HQS Constraints			
$B \to D_1^{1/2}$	$0.57^{+0.00}_{-0.09}$	$-0.066^{+0.013}_{-0.001}$	$0.071^{+0.000}_{-0.015}$
$B \to D_1^{3/2}$	$-1.20^{+0.05}_{-0.00}$	$-0.092^{+0.012}_{-0.001}$	$-0.067^{+0.010}_{-0.001}$
LQCD based estimates			
$B \to D_1^{1/2}$	0.54 ± 0.06	-0.066 ± 0.006	0.066 ± 0.006
$B \to D_1^{3/2}$	-0.64 ± 0.03	-0.057 ± 0.002	-0.036 ± 0.001

4.3. The $B \to A/A'$ transition form factors in ISGW II quark model in HQS

Aforementioned, the ISGW II quark model incorporates *HQS constraints* and employs HQET for systematical treatment of the perturbative QCD corrections and $1/m_Q$ expansion. The ISGW II model defines the form factors $\ell_{1/2(3/2)}$, $c_{+1/2(3/2)}$, $c_{-1/2(3/2)}$, and $q_{1/2(3/2)}$ analogous to (25) under the heavy quark spin S_Q coupling (the exact expressions for the form factor can be found in Appendix C of the original work [6]):

$$\begin{aligned}
D_1^{1/2}(P_A)|V_\mu|B(P_B)\rangle &= i[\ell_{1/2}(q^2)\varepsilon^*_\mu + c_+^{1/2}(q^2)(\varepsilon^* \cdot P_B)(P_B + P_A)_\mu \\
&\quad + c_-^{1/2}(q^2)(\varepsilon^* \cdot P_B)(P_B - P_A)_\mu], \\
D_1^{1/2}(P_A)|A_\mu|B(P_B)\rangle &= -q_{1/2}(q^2)\epsilon_{\mu\nu\rho\sigma}\varepsilon^{*\nu}(P_B + P_A)^\rho(P_B - P_A)^\sigma, \\
D_1^{3/2}(P_A)|V_\mu|B(P_B)\rangle &= i[\ell_{3/2}(q^2)\varepsilon^*_\mu + c_+^{3/2}(q^2)(\varepsilon^* \cdot P_B)(P_B + P_A)_\mu \\
&\quad + c_-^{3/2}(q^2)(\varepsilon^* \cdot P_B)(P_B - P_A)_\mu], \\
D_1^{3/2}(P_A)|A_\mu|B(P_B)\rangle &= -q_{3/2}(q^2)\epsilon_{\mu\nu\rho\sigma}\varepsilon^{*\nu}(P_B + P_A)^\rho(P_B - P_A)^\sigma.
\end{aligned} \tag{30}$$

The calculated formfactors are given in the rows 3 and 4 of Table 5.

4.4. LQCD inspired form factors in HQS

The biggest advantage of the HQS is that, in the infinite mass limit, all the heavy to heavy transition form factors are reduced to some universal Isgur-Wise functions, $\xi(\omega)$, $\tau_{1/2}(\omega)$, and $\tau_{3/2}(\omega)$ (for extensive review see [59]). The function $\xi(\omega)$ occurs in $s-$wave to $s-$wave transitions while $\tau_{1/2}(\omega)$ and $\tau_{3/2}(\omega)$ are involved in $s-$wave to $p-$wave transitions, thus, the matrix elements of $B \to D_1^{1/2}$, $D_1^{3/2}$ transitions in the heavy quark limit are of the form:

$$\begin{aligned}
\langle D_1^{1/2}(v',\varepsilon)|V_\mu|B(v)\rangle &= -i\,2\tau_{1/2}(\omega)\Big[(1-\omega)\varepsilon^*_\mu + (\varepsilon^*\cdot v)v'_\mu\Big],\\
\langle D_1^{1/2}(v',\varepsilon)|A_\mu|B(v)\rangle &= -2\tau_{1/2}(\omega)\epsilon_{\mu\nu\alpha\beta}\varepsilon^{*\nu}v'^{\alpha}v^{\beta},\\
\langle D_1^{3/2}(v',\varepsilon)|V_\mu|B(v)\rangle &= i\frac{1}{\sqrt{2}}\tau_{3/2}(\omega)\Big\{(1-\omega^2)\varepsilon^*_\mu - (\varepsilon^*\cdot v)[3v_\mu + (2-\omega)v'_\mu]\Big\},\\
\langle D_1^{3/2}(v',\varepsilon)|A_\mu|B(v)\rangle &= \frac{1}{\sqrt{2}}\tau_{3/2}(\omega)(1+\omega)\epsilon_{\mu\nu\alpha\beta}\varepsilon^{*\nu}v'^{\alpha}v^{\beta},
\end{aligned}\tag{31}$$

where $\omega(\equiv v\cdot v') = (m_B^2 + m_{D_1}^2 - q^2)/(2m_B m_{D_1})$. The form factors for $B \to D_1^{1/2}$ transition are related to $\tau_{1/2}(\omega)$ as follows [9]:

$$\begin{aligned}
\ell_{1/2}(q^2) &= 2\sqrt{m_B m_{D_1^{1/2}}}\,(\omega-1)\,\tau_{1/2}(\omega),\\
q_{1/2}(q^2) &= \frac{\tau_{1/2}(\omega)}{\sqrt{m_B m_{D_1^{1/2}}}},\\
c_+^{1/2}(q^2) - c_-^{1/2}(q^2) &= -\frac{2\tau_{1/2}(\omega)}{\sqrt{m_B m_{D_1^{1/2}}}},\\
c_+^{1/2}(q^2) + c_-^{1/2}(q^2) &= 0.
\end{aligned}\tag{32}$$

Similarly, the form factors for $B \to D_1^{3/2}$ transition are related to $\tau_{3/2}(\omega)$ by

$$\begin{aligned}
\ell_{3/2}(q^2) &= -\sqrt{\frac{m_B m_{D_1^{3/2}}}{2}}(\omega^2-1)\tau_{3/2}(\omega),\\
c_+^{3/2}(q^2) + c_-^{3/2}(q^2) &= -3\sqrt{\frac{m_{D_1^{3/2}}}{2m_B^3}}\tau_{3/2}(\omega),\\
c_-^{3/2}(q^2) - c_-^{3/2}(q^2) &= \sqrt{\frac{m_{D_1^{3/2}}}{2m_B^3}}(\omega-2)\tau_{3/2}(\omega),\\
q_{3/2}(q^2) &= -\frac{1+\omega}{2\sqrt{2}}\frac{\tau_{3/2}(\omega)}{\sqrt{m_B m_{D_1^{3/2}}}}.
\end{aligned}\tag{33}$$

It is desirable to check the behavior of the form factors (in any model) in heavy quark limit to see the consistency of the results. Conventionally, the Isgur-Wise functions are parameterized as a function of ω and shape parameter ρ^2.

In the present work, we follow M. Atoui et al. [36,37] *lattice QCD framework* based results to extract the qualitative estimate of the $B \to D_1^{1/2}, D_1^{3/2}$ form factors. M. Atoui et al. has parameterized the Isgur-Wise function $\tau_{3/2}$ using the Bakamjian-Thomas (BT) model [59] as :

$$\tau_{3/2}(\omega) = \tau_{3/2}(1) \left(\frac{2}{1+w}\right)^{2\rho^2_{3/2}}. \tag{34}$$

In [59], following ISGW, $\tau_{3/2}(1) \simeq 0.54$ and $\rho^2_{3/2} \simeq 1.50$ has been used. The same shape parametrization can be used for $\tau_{1/2}$:

$$\tau_{1/2}(\omega) = \tau_{1/2}(1) \left(\frac{2}{1+w}\right)^{2\rho^2_{1/2}}, \tag{35}$$

with $\rho^2_{1/2} \simeq 0.83$ [59]. It is worth noticing that ρ^2, $\tau_{1/2}$, and $\tau_{3/2}$ are related by Uraltsev [60] and Bjorken [61] sum rules, respectively:

$$\sum_n |\tau^{(n)}_{3/2}(1)|^2 - \sum_n |\tau^{(n)}_{1/2}(1)|^2 = \frac{1}{4}, \tag{36}$$

$$\rho^2 = \frac{1}{4} + \sum_n |\tau^{(n)}_{1/2}(1)|^2 + 2\sum_n |\tau^{(n)}_{3/2}(1)|^2, \tag{37}$$

where $\tau_i(1)$ represents the values at zero recoil ($\omega = 1$) and n stands for the radial excitations. It is well established that in these sum rules the ground state dominates. B. Blossier et al. [35], in lattice QCD based analyses, has shown that the Uraltsev's sum rule receives $\sim 80\%$ contributions from the ground state, consequently, they obtained:

$$\tau_{1/2}(1) = 0.30 \pm 0.03, \qquad \tau_{3/2}(1) = 0.53 \pm 0.02, \tag{38}$$

which are in reasonably good agreement with the other theoretical works (e.g. see [29,62]). Moreover, their results based on the unquenched computations and better analyses procedure are expected to be more reliable. Thus, using the lattice QCD results (38) and HQS based relations (32)-(33), we obtain the qualitative guess for $B \to D_1^{1/2}, D_1^{3/2}$ transition form factors. The numerical values of the calculated form factors are given in rows 6 and 7 of Table 5. It may be noted that the $B \to D^{1/2}$ transition form factors in this case are comparable to the ISGW II (in HQS), however, the $B \to D^{3/2}$ transition form factors are much smaller (roughly by a factor of 2). We wish to remark that it may appear a phenomenological simplification to extract the form factors directly from the HQS relations and Isgur-Wise functions $\tau_{1/2}(1)$, $\tau_{3/2}(1)$. Also, it has already been pointed out in the literature that $1/m_Q$ corrections may be large and play essential role in heavy flavor physics. However, at the same time, the advantage of lattice QCD to have a systematic approach leading to the true results of QCD cannot be ignored. Moreover, with improvements in LQCD calculations, the errors could be estimated in near future. Further, it may be noted that the estimates drawn from the lattice QCD for $\tau_{1/2}(\omega)$ and $\tau_{3/2}(\omega)$,

$$|\tau_{1/2}(1.32)| = 0.23 \qquad |\tau_{3/2}(1.32)| = 0.34 \tag{39}$$

are in good agreement with the results extracted from the experimental data [19,21] and other theoretical models (see for details [62]).

For $B \to P$ transition, we use the lattice QCD form factors [42–44] as shown in column 2 of Table 6. These form factors are consistent with the LCSR values, thus we use the recent LCSR based form factors for $B \to \eta^{(\prime)}$ in our calculations [45].

Table 6
LQCD based form factors of $B(0^-) \to P(0^-)$ transitions.

Transition	$F_0^{BP}(0)$
$B \to \pi$	0.27 ± 0.05
$B \to K$	0.32 ± 0.06
$B \to D$	0.66 ± 0.03
$B \to \eta/\eta'$	$0.17 \pm 0.04/0.13 \pm 0.03$

Table 7
Branching ratios for $B \to PA$ decays in CKM-favored ($\Delta b = 1, \Delta C = 1, \Delta S = 0$) mode. Numbers in [ ] are experimental values.

Decays	Branching ratios
$B^- \to \pi^- D_1^0$	$(7.0 \pm 0.8) \times 10^{-4}[(7.5 \pm 1.7) \times 10^{-4}]$
$B^- \to \pi^- \underline{D}_1^0$	$(2.0 \pm 0.4) \times 10^{-3}[(1.5 \pm 0.6) \times 10^{-3}]$
$B^- \to D^0 a_1^-$	$(1.2 \pm 0.1) \times 10^{-2}[(4.0 \pm 4.0) \times 10^{-3}]$
$B^- \to D^0 b_1^-$	$(1.3^{+0.7}_{-0.2}) \times 10^{-4}$
$\bar{B}^0 \to \pi^0 D_1^0$	$(4.3 \pm 1.8) \times 10^{-8}$
$\bar{B}^0 \to \pi^0 \underline{D}_1^0$	$(5.4 \pm 1.9) \times 10^{-6}$
$\bar{B}^0 \to \pi^- D_1^+$	$(6.4 \pm 0.7) \times 10^{-4}$
$\bar{B}^0 \to \pi^- \underline{D}_1^+$	$(1.6 \pm 0.3) \times 10^{-3}$
$\bar{B}^0 \to \eta D_1^0$	$(1.0 \pm 3.0) \times 10^{-8}$
$\bar{B}^0 \to \eta \underline{D}_1^0$	$(1.2 \pm 0.4) \times 10^{-6}$
$\bar{B}^0 \to \eta' D_1^0$	$(3.3 \pm 1.5) \times 10^{-9}$
$\bar{B}^0 \to \eta' \underline{D}_1^0$	$(4.1 \pm 1.9) \times 10^{-7}$
$\bar{B}^0 \to D^+ a_1^-$	$(8.5 \pm 0.8) \times 10^{-3}$ $[(6.0 \pm 3.3) \times 10^{-3}]$
$\bar{B}^0 \to D^+ b_1^-$	$(7.6 \pm 0.6) \times 10^{-8}$
$\bar{B}^0 \to D^0 a_1^0$	$(1.2^{+0.5}_{-0.2}) \times 10^{-4}$
$\bar{B}^0 \to D^0 f_1$	$(1.1^{+0.5}_{-0.2}) \times 10^{-4}$
$\bar{B}^0 \to D^0 b_1^0$	$(6.4^{+3.7}_{-1.1}) \times 10^{-5}$
$\bar{B}^0 \to D^0 h_1$	$(6.8^{+3.4}_{-1.2}) \times 10^{-5}$

5. Numerical results and discussions

We have calculated the branching ratios (which are expected to be tree dominant) of B and $\bar{B}^0$ mesons for the various decays in CKM-favored and CKM-suppressed modes. The results based on *scenario-I* in ISGW II model (without heavy quark symmetry constraints) are given in Tables 7, 8, 9, and 10. In *scenario-II*, we have obtained the form factors and branching ratios for the decays involving charm meson in the light of heavy quark symmetry constraints (in ISGW II and LQCD) are given in Tables 11 and 12. Our results are as follows:

Scenario-I: $B \to PA$ decays in ISGW II quark model

1. $\Delta b = 1, \Delta C = 1, \Delta S = 0$ *mode:*

$B^- \to D^0 a_1^-$, $\bar{B}^0 \to D^+ a_1^-$, $B^- \to \pi^- \underline{D}_1^0$, and $\bar{B}^0 \to \pi^- \underline{D}_1^+$ are the dominant decays with branching ratios of the order of $\mathcal{O}(10^{-2}) \sim \mathcal{O}(10^{-3})$. The highest branching ratio is $B(B^- \to$

Table 8
Branching ratios for $B \to PA$ decays in $\Delta b = 1, \Delta C = 1, \Delta S = -1$ mode.

Decays	Branching ratios
$B^- \to K^- D_1^0$	$(5.0 \pm 0.6) \times 10^{-5}$
$B^- \to K^- \underline{D}_1^0$	$(1.4 \pm 0.3) \times 10^{-4}$
$B^- \to D^0 K_1^-$	$(5.5 \pm 0.4) \times 10^{-4}$
$B^- \to D^0 \underline{K}_1^-$	$(6.0 \pm 0.5) \times 10^{-4}$
$\bar{B}^0 \to \bar{K}^0 D_1^0$	$(5.3 \pm 2.0) \times 10^{-9}$
$\bar{B}^0 \to \bar{K}^0 \underline{D}_1^0$	$(7.5 \pm 3.0) \times 10^{-7}$
$\bar{B}^0 \to K^- D_1^+$	$(4.6 \pm 0.5) \times 10^{-5}$
$\bar{B}^0 \to K^- \underline{D}_1^+$	$(1.1 \pm 0.1) \times 10^{-4}$
$\bar{B}^0 \to D^+ K_1^-$	$(3.6 \pm 0.3) \times 10^{-4}$
$\bar{B}^0 \to D^+ \underline{K}_1^-$	$(5.2 \pm 0.4) \times 10^{-4}$
$\bar{B}^0 \to D^0 \bar{K}_1^0$	$(1.3 \pm 0.1) \times 10^{-5}$
$\bar{B}^0 \to D^0 \underline{\bar{K}}_1^0$	$(6.8 \pm 0.6) \times 10^{-7}$

Table 9
Branching ratios for $B \to PA$ decays in $\Delta b = 1, \Delta C = -1, \Delta S = -1$ mode. The numbers in [ ] are experimental values.

Decays	Branching ratios
$B^- \to \pi^0 D_{s1}^-$	$(3.2 \pm 1.3) \times 10^{-6}$
$B^- \to \pi^0 \underline{D}_{s1}^-$	$(1.1 \pm 0.5) \times 10^{-6}$
$B^- \to \eta D_{s1}^-$	$(7.1 \pm 2.5) \times 10^{-7}$
$B^- \to \eta \underline{D}_{s1}^-$	$(2.5 \pm 0.9) \times 10^{-7}$
$B^- \to K^- \bar{D}_1^0$	$(2.4 \pm 0.9) \times 10^{-10}$
$B^- \to K^- \underline{\bar{D}}_1^0$	$(1.6 \pm 0.6) \times 10^{-7}$
$B^- \to \eta' D_{s1}^-$	$(2.4 \pm 1.1) \times 10^{-7}$
$B^- \to \eta' \underline{D}_{s1}^-$	$(8.5 \pm 0.4) \times 10^{-8}$
$B^- \to \bar{D}^0 K_1^-$	$(2.2 \pm 0.1) \times 10^{-6}$
$B^- \to \bar{D}^0 \underline{K}_1^-$	$(1.1 \pm 0.1) \times 10^{-7}$
$B^- \to D_s^- a_1^0$	$(1.0^{+0.6}_{-0.1}) \times 10^{-4}$ [$< 1.8 \times 10^{-3}$]
$B^- \to D_s^- f_1$	$(1.0^{+0.5}_{-0.1}) \times 10^{-4}$
$B^- \to D_s^- b_1^0$	$(5.8^{+3.4}_{-0.9}) \times 10^{-5}$
$B^- \to D_s^- h_1$	$(6.1^{+4.0}_{-1.0}) \times 10^{-5}$
$\bar{B}^0 \to \pi^+ D_{s1}^-$	$(5.9 \pm 2.8) \times 10^{-6}$
$\bar{B}^0 \to \pi^+ \underline{D}_{s1}^-$	$(2.1 \pm 0.9) \times 10^{-6}$
$\bar{B}^0 \to \bar{K}^0 \bar{D}_1^0$	$(2.3 \pm 0.8) \times 10^{-10}$
$\bar{B}^0 \to \bar{K}^0 \underline{\bar{D}}_1^0$	$(1.5 \pm 0.8) \times 10^{-7}$
$\bar{B}^0 \to \bar{D}^0 \bar{K}_1^0$	$(2.0 \pm 0.1) \times 10^{-6}$
$\bar{B}^0 \to \bar{D}^0 \underline{\bar{K}}_1^0$	$(1.0 \pm 0.1) \times 10^{-7}$
$\bar{B}^0 \to D_s^- a_1^+$	$(1.9^{+1.1}_{-0.2}) \times 10^{-4}$ [$< 2.1 \times 10^{-3}$]
$\bar{B}^0 \to D_s^- b_1^+$	$(1.1^{+0.6}_{-0.1}) \times 10^{-4}$

Table 10
Branching ratios for $B \to PA$ decays in $\Delta b = 1, \Delta C = -1, \Delta S = 0$ mode.

Decays	Branching ratios
$B^- \to \pi^0 D_1^-$	$(4.9 \pm 2.1) \times 10^{-10}$
$B^- \to \pi^0 \underline{D}_1^-$	$(2.5 \pm 1.1) \times 10^{-7}$
$B^- \to \pi^- \bar{D}_1^0$	$(1.2 \pm 0.5) \times 10^{-11}$
$B^- \to \pi^- \underline{\bar{D}}_1^0$	$(6.1 \pm 2.7) \times 10^{-9}$
$B^- \to \eta D_1^-$	$(1.1 \pm 0.4) \times 10^{-10}$
$B^- \to \eta \underline{D}_1^-$	$(5.7 \pm 2.0) \times 10^{-8}$
$B^- \to \eta' D_1^-$	$(3.7 \pm 1.7) \times 10^{-11}$
$B^- \to \eta' \underline{D}_1^-$	$(1.9 \pm 0.9) \times 10^{-8}$
$B^- \to D^- a_1^0$	$(4.1^{+2.4}_{-0.5}) \times 10^{-6}$
$B^- \to D^- f_1$	$(3.8^{+2.2}_{-0.5}) \times 10^{-6}$
$B^- \to D^- b_1^0$	$(2.2^{+1.3}_{-0.3}) \times 10^{-6}$
$B^- \to D^- h_1$	$(2.4^{+1.6}_{-0.4}) \times 10^{-6}$
$B^- \to \bar{D}^0 a_1^-$	$(1.0^{+0.7}_{-0.1}) \times 10^{-7}$
$B^- \to \bar{D}^0 b_1^-$	$(5.6^{+3.9}_{-0.9}) \times 10^{-8}$
$\bar{B}^0 \to \pi^+ D_1^-$	$(9.1 \pm 4.0) \times 10^{-10}$
$\bar{B}^0 \to \pi^+ \underline{D}_1^-$	$(4.7 \pm 2.0) \times 10^{-7}$
$\bar{B}^0 \to \pi^0 \bar{D}_1^0$	$(5.5 \pm 2.4) \times 10^{-12}$
$\bar{B}^0 \to \pi^0 \underline{\bar{D}}_1^0$	$(2.8 \pm 1.2) \times 10^{-9}$
$\bar{B}^0 \to \eta \bar{D}_1^0$	$(1.2 \pm 0.5) \times 10^{-12}$
$\bar{B}^0 \to \eta \underline{\bar{D}}_1^0$	$(6.4 \pm 2.2) \times 10^{-10}$
$\bar{B}^0 \to \eta' \bar{D}_1^0$	$(4.2 \pm 1.9) \times 10^{-13}$
$\bar{B}^0 \to \eta' \underline{\bar{D}}_1^0$	$(2.2 \pm 1.1) \times 10^{-10}$
$\bar{B}^0 \to D^- a_1^+$	$(7.7^{+4.3}_{-1.0}) \times 10^{-6}$
$\bar{B}^0 \to D^- b_1^+$	$(4.2^{+2.5}_{-0.7}) \times 10^{-6}$
$\bar{B}^0 \to \bar{D}^0 a_1^0$	$(4.9^{+3.1}_{-0.7}) \times 10^{-8}$
$\bar{B}^0 \to \bar{D}^0 f_1$	$(4.5^{+2.8}_{-0.7}) \times 10^{-8}$
$\bar{B}^0 \to \bar{D}^0 b_1^0$	$(2.6^{+1.8}_{-0.4}) \times 10^{-8}$
$\bar{B}^0 \to \bar{D}^0 h_1$	$(2.8^{+2.2}_{-0.5}) \times 10^{-8}$

$D^0 a_1^-) = (1.2 \pm 0.1) \times 10^{-2}$. Four of the decay channels are experimentally measured which are discussed as follows:

i. For $\bar{B} \to \pi D_1$ type decay modes, the branching ratios of Class III decays are

$$B(B^- \to \pi^- \underline{D}_1^0) = (2.0 \pm 0.4) \times 10^{-3} \qquad (1.5 \pm 0.6) \times 10^{-3} \text{ [41] } (Expt);$$
$$B(B^- \to \pi^- D_1^0) = (7.0 \pm 0.8) \times 10^{-4} \qquad (7.5 \pm 1.7) \times 10^{-4} \text{ [19] } (Expt).$$

The calculated branching ratios are in good agreement with the available experimental values. Fig. 1 shows the variation of branching ratios, $B(B^- \to \pi^- \underline{D}_1^0)$ and $B(B^- \to \pi^- D_1^0)$, w.r.t. mixing angle, θ_{D_1}, that supports our choice of positive mixing angle. The effect of the positive mixing angle is such that both the decay amplitudes receive contributions from the constructive interference between the color-favored and color-suppressed transitions. Both,

Table 11
HQS constrained branching ratios for $B \to PA$ decays in CKM-favored mode. The values in [ ] are experimental values.

Decays	This work		[18,19]
	ISGW	LQCD	
$\Delta b = 1, \Delta C = 1, \Delta S = 0$			
$B^- \to \pi^- D_1^0$	$(4.1^{+1.7}_{-1.1}) \times 10^{-4}$	$(5.7 \pm 2.0) \times 10^{-4}$ $[(7.5 \pm 1.7) \times 10^{-4}]$	3.6×10^{-4}
$B^- \to \pi^- \underline{D}_1^0$	$(2.3 \pm 0.3) \times 10^{-3}$	$(0.9 \pm 0.1) \times 10^{-3}$ $[(1.5 \pm 0.6) \times 10^{-3}]$	1.1×10^{-3}
$\bar{B}^0 \to \pi^0 D_1^0$	$(6.9 \pm 2.8) \times 10^{-5}$	$(6.9 \pm 2.8) \times 10^{-5}$	1.4×10^{-4}
$\bar{B}^0 \to \pi^0 \underline{D}_1^0$	$(3.6 \pm 1.5) \times 10^{-6}$	$(3.6 \pm 1.5) \times 10^{-6}$	3.5×10^{-5}
$\bar{B}^0 \to \pi^- D_1^+$	$(0.6 \pm 0.2) \times 10^{-4}$	$(1.3 \pm 0.3) \times 10^{-4}$	0.8×10^{-4}
$\bar{B}^0 \to \pi^- \underline{D}_1^+$	$(2.6 \pm 0.3) \times 10^{-3}$	$(1.0 \pm 0.1) \times 10^{-3}$	1.0×10^{-3}
$\bar{B}^0 \to \eta D_1^0$	$(1.5 \pm 0.5) \times 10^{-5}$	$(1.5 \pm 0.5) \times 10^{-5}$	–
$\bar{B}^0 \to \eta \underline{D}_1^0$	$(7.9 \pm 2.8) \times 10^{-7}$	$(7.9 \pm 2.8) \times 10^{-7}$	–
$\bar{B}^0 \to \eta' D_1^0$	$(5.3 \pm 2.5) \times 10^{-6}$	$(5.3 \pm 2.5) \times 10^{-6}$	–
$\bar{B}^0 \to \eta' \underline{D}_1^0$	$(2.7 \pm 1.3) \times 10^{-7}$	$(2.7 \pm 1.3) \times 10^{-7}$	–

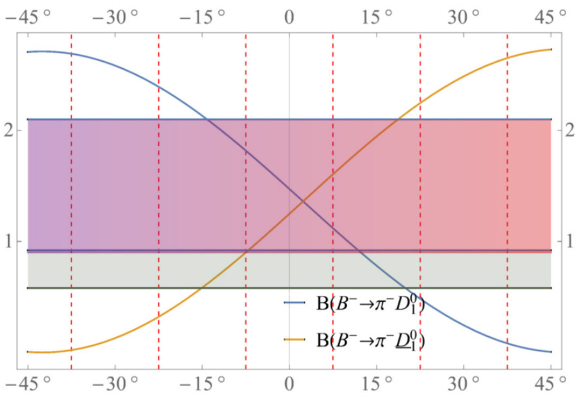

Fig. 1. Plot of the branching ratios vs mixing angle. Experimental branching ratio ranges are shown as shaded regions: gray for $B(B^- \to \pi^- D_1^0)$ and colored for $B(B^- \to \pi^- \underline{D}_1^0)$.

$B^- \to \pi^- \underline{D}_1^0$ and $B^- \to \pi^- D_1^0$, decays receive dominant contributions from the color-favored transition, however, the color-suppressed contribution in later are such small that it, roughly, behave like a color allowed decay. On the other hand, branching ratios of the (Class I) color allowed decays resulting from the internal W-emission tree processes are $B(\bar{B}^0 \to \pi^- \underline{D}_1^+)$= $(1.6 \pm 0.3) \times 10^{-3}$ and $B(\bar{B}^0 \to \pi^- D_1^+) = (6.4 \pm 0.7) \times 10^{-4}$.

ii. For $\bar{B} \to Da$ type decays, the calculated branching ratios are:

$$B(\bar{B}^0 \to D^+ a_1^-) = (0.85 \pm 0.08) \times 10^{-2} \qquad (0.60 \pm 0.33) \times 10^{-2} \text{ [41] } (Expt);$$
$$B(B^- \to D^0 a_1^-) = (1.2 \pm 0.1) \times 10^{-2} \qquad (4.0 \pm 4.0) \times 10^{-3} \text{ [41] } (Expt).$$

Both the calculated branching ratios are consistent with the experimental results within the errors. The most dominant $\bar{B}^0 \to D^+ a_1^-$ decay receive contribution from the color-favored transition only, however, the $B^- \to D^0 a_1^-$ decay get contributions through the destructive interference between the color-favored and color-suppressed transitions resulting in smaller branching ratio. The next order decays: $\bar{B}^0 \to D^0 b_1^- / D^0 a_1^0 / D^0 f_1 / \pi^- D_1^+$ have branching ratios of the $\mathcal{O}(10^{-4})$ well withing the reach of current experiments.

2. $\Delta b = 1, \Delta C = -1, \Delta S = -1$ *mode:*

i. The dominant decays in present mode have $B(\bar{B}^0 \to D_s^- a_1^+) = (1.9^{+1.1}_{-0.2}) \times 10^{-4}$, $B(B^- \to D_s^- f_1) = (1.0^{+0.5}_{-0.1}) \times 10^{-4}$, $B(B^- \to D_s^- a_1^0) = (1.0^{+0.6}_{-0.1}) \times 10^{-4}$, and $B(\bar{B}^0 \to D_s^- b_1^+) = (1.1^{+0.6}_{-0.1}) \times 10^{-4}$.

ii. Calculated branching ratios for the $\bar{B}^0 \to D_s^- a_1^+$ and $B^- \to D_s^- a_1^0$ decays are consistent with the experimental upper limits [41] $< 1.8 \times 10^{-3}$ and $< 2.2 \times 10^{-3}$.

3. $\Delta b = 1, \Delta C = 1, \Delta S = -1$ *mode:*

The branching ratios for these decays range from $(10^{-4}) \sim (10^{-9})$, as shown in Table 7. Some of these decays could be of experimental importance. Decays $B^- \to \bar{K}^0 D_1^- / \bar{K}^0 \underline{D}_1^- / D^- \bar{K}_1^0 / D^- \underline{\bar{K}}_1^0 / D_s^- f_1' / D_s^- h_1'$ are forbidden in the present analysis. Annihilation and FSIs may generate these decays.

4. $\Delta b = 1, \Delta C = -1, \Delta S = 0$ *mode:*

The decay channels in $\Delta b = 1, \Delta C = -1, \Delta S = 0$ mode are highly suppressed with the branching ratios of $\mathcal{O}(10^{-6}) \sim \mathcal{O}(10^{-13})$.

Scenario-II: based on heavy quark symmetry constraints in ISGWII and LQCD

To compare our results with the existing theoretical analyses, we have calculated the branching ratios of B meson decay to charm mesons in the light of heavy quark symmetry constraints. We follow two different approaches to evaluate the form factors involved in $B \to D_1^{1/2}, D_1^{3/2}$ transitions. *Firstly*, we employ the ISGW II quark model with HQS constraints (for details see [5,6]) to calculate these form factors as given in Table 5. *Secondly*, we use the recent lattice QCD results for $\tau_{1/2}(1)$ and $\tau_{3/2}(1)$ to get the qualitative estimates of these form factors as shown in Table 5. It may be noted that the signs of the calculated form factors are consistent with the heavy quark expectations. For $B \to P$ transition, we use the form factors from the lattice QCD framework (Table 6). The values of the decay constants used are $f_{D_1^{1/2}} = 0.179$ GeV and $f_{D_1^{3/2}} = -0.053$ GeV [38]. The experimentally determined $D_1^{1/2} - D_1^{3/2}$ mixing angle $-5.7°$ [48] is used to calculate the branching ratios. As we have already seen in *scenario-I*, the color-favored and color-suppressed diagrams can interfere constructively or destructively based on their relative signs. After the signs of form factors and decay constants being fixed in theory, the relative signs of a_1 and a_2 are very important to explain the experimental data. At $N_c = 3$, both a_1 and a_2 are positive as shown in (14), which gives:

$$B(B^- \to \pi^- \underline{D}_1^0) = 3.1 \times 10^{-3} \qquad (1.5 \pm 0.6) \times 10^{-3}|_{Expt};$$
$$B(B^- \to \pi^- D_1^0) = 1.4 \times 10^{-5} \qquad (7.5 \pm 1.7) \times 10^{-4}|_{Expt},$$

for ISGW model within HQS. Being Class III modes, these decay channels receive contributions from both the color-favored and color-suppressed tree level diagrams. The color-favored

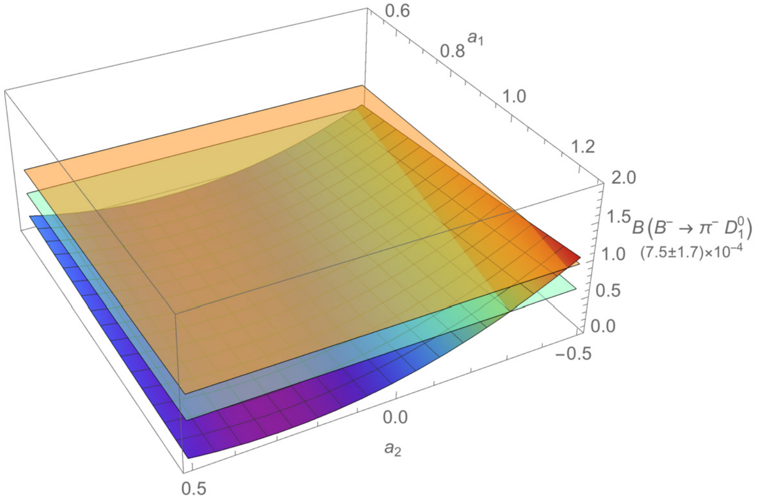

Fig. 2. The branching ratio of $B^- \to \pi^- D_1^0$ decay w.r.t. the parameters a_1 and a_2 in heavy quark symmetry constraints. The intersecting parallel planes represent the upper and lower limits of experimental branching ratio [19].

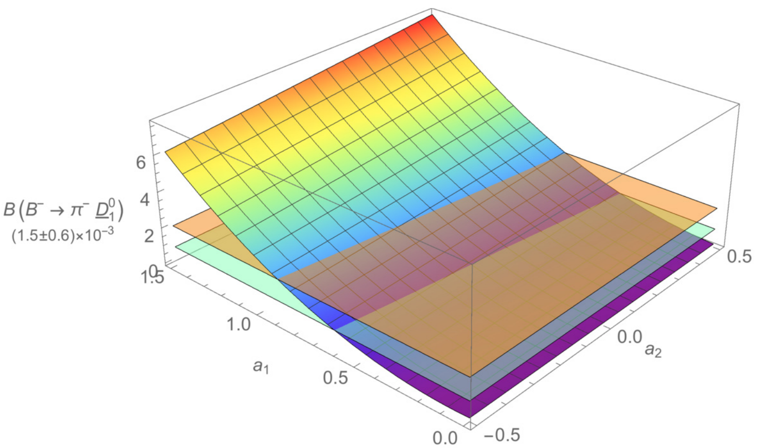

Fig. 3. The branching ratio of $B^- \to \pi^- \underline{D}_1^0$ decay w.r.t. the parameters a_1 and a_2 in heavy quark symmetry constraints. The intersecting parallel planes represent the upper and lower limits of experimental branching ratio [41].

and -suppressed amplitudes in $B^- \to \pi^- \underline{D}_1^0$ interfere constructively, while they interfere destructively for $B^- \to \pi^- D_1^0$. It is worth pointing out that the color-suppressed contributions in the $B^- \to \pi^- D_1^0$ decay are comparable to the color-favored amplitudes, however, these contributions are *negligibly small* in $B^- \to \pi^- \underline{D}_1^0$ decay. Therefore, a careful investigation of the branching ratio for $B^- \to \pi^- D_1^0$ decay, and its comparison with experiment demands negative sign and larger magnitude of a_2.

In order to get a clearer picture of effective dependence on a_1 and a_2, we plot the theoretical branching ratios of $B^- \to \pi^- D_1^0$ and $B^- \to \pi^- \underline{D}_1^0$ decays w.r.t. the parameters a_1 and a_2 as shown in Figs. 2 and 3, respectively. These plots show that the experimental branching ratio for $B^- \to \pi^- D_1^0$ decay demands effectively larger magnitude and negative sign for the color-suppressed amplitude proportional to the parameter a_2 and relatively, smaller magnitude for the color-favored amplitude proportional to a_1. Therefore, we use effective a_1^{eff} and a_2^{eff}, such that, a_1^{eff} should have smaller magnitude ($|a_1^{eff}| < |a_1|$) with positive sign and a_2^{eff} should have larger magnitude ($|a_2^{eff}| > |a_2|$) with negative sign. It is interesting to note that the same choice of magnitude and signs of the parameters, a_1^{eff} and a_2^{eff}, can also be used in case of $B^- \to \pi^- \underline{D}_1^0$ decay for which experimental branching ratio shows a large overlap region (see Fig. 3) with respect to the color-suppressed and color-favored contributions. Here, $B^- \to \pi^- \underline{D}_1^0$ decay is nearly independent of the color-suppressed contributions. As mentioned earlier, the experimental data for $B \to D\pi$ yields $|a_2^{eff}/a_1^{eff}| \sim (0.45 - 0.65)e^{\pm i60}$ [53]. Also, the color-suppression parameter, a_2^{eff}, is hard to calculate for $\bar{B} \to D^{**}\pi$ type decays in the QCD factorization due to D mesons being heavy and slow cannot be decoupled from $(B\pi)$ system. Moreover, in the absence of experimental information on $B \to D^{**}\pi$ decays, it is difficult to explain the relative phase between $|a_1^{eff}|$ and $|a_2^{eff}|$. Thus, acquiring the estimate of color-suppression is even more difficult task in the absence of more and precise experimental results. Therefore, in order to explain the experimental results, we fix (for HQS calculations hereafter)

$$a_1^{eff} \simeq 1.0 \text{ and } \quad a_2^{eff} \simeq -0.30 \tag{40}$$

based on the non-perturbative corrections [21,50–52]. Following this, we get the branching ratios:

$$B(B^- \to \pi^- \underline{D}_1^0) = (2.3 \pm 0.3) \times 10^{-3} \qquad B(B^- \to \pi^- D_1^0) = (4.1^{+1.7}_{-1.1}) \times 10^{-4}.$$

The branching ratios for $B^- \to \pi^- \underline{D}_1^0$ and $B^- \to \pi^- D_1^0$ are in fair agreement with the experimental expectations within the errors. Since, $B^- \to \pi^- \underline{D}_1^0$ get dominant contribution from the color-favored amplitude, the effect of destructive interference is negligibly small. In fact, its branching ratio is equivalent to $\bar{B}^0 \to \pi^- \underline{D}_1^+$ which is a class I decay. However, the $B^- \to \pi^- D_1^0$ decay receives comparable contribution from both the color-favored and -suppressed amplitudes, despite of constructive interference $B^- \to \pi^- D_1^0$ decay have, relatively, smaller branching ratio. The Class I - $\bar{B}^0 \to \pi \underline{D}_1$ type decays which receive contribution from the color-favored diagrams only, have branching ratios $B(\bar{B}^0 \to \pi^- \underline{D}_1^+) = (2.6 \pm 0.3) \times 10^{-3}$ and $B(\bar{B}^0 \to \pi^- D_1^+) = (0.6 \pm 0.2) \times 10^{-4}$, respectively. Interestingly, H. Y. Cheng [19] use $\left| a_2^{eff} \middle/ a_1^{eff} \right| = 0.53$ obtained from the experimental data of $B \to D\pi$ which leads to $a_1^{eff} = 0.88$ and $a_2^{eff} = -0.47$. Once taken in to account, we get

$$B(B^- \to \pi^- \underline{D}_1^0) = 2.0 \times 10^{-3}, \qquad B(B^- \to \pi^- D_1^0) = 7.3 \times 10^{-4},$$

which are in good agreement with the experimental data. The branching ratios of $\bar{B}^0 \to \pi \underline{D}_1$ modes become: $B(\bar{B}^0 \to \pi^- \underline{D}_1^+) = 2.2 \times 10^{-3}$ and $B(\bar{B}^0 \to \pi^- D_1^+) = 0.6 \times 10^{-4}$, respectively.

The small inconsistency with the experimental results point to the fact that, in Class III decays, contribution from the constructive and destructive interferences of the color-favored and color-suppressed transitions are important and cannot be ignored. We wish to remark that, in heavy quark limit [47], the contributions from color-suppressed amplitudes are further suppressed by a factor of $1/m_Q$. However, the mismatch with experiment in case of $B^- \to \pi^- D_1^0$ decay indicates large contribution from the color-suppressed amplitude. Also, the implications of HQS framework are such that the theoretical results would become merely independent of the color-suppressed contributions. Therefore, yielding the relations:

$$B(B^- \to \pi^- \underline{D}_1^0) = B(\bar{B}^0 \to \pi^- \underline{D}_1^+), \tag{41}$$
$$B(B^- \to \pi^- D_1^0) = B(\bar{B}^0 \to \pi^- D_1^+), \tag{42}$$

in heavy quark limit. However, these relations may not be satisfied in some of the cases owing to relatively larger contributions from the color-suppressed amplitudes. Thus, the experimental measurement of the ratio $B(B^- \to \pi^- D_1^0)/B(\bar{B}^0 \to \pi^- D_1^+)$ could provide useful information on relative signs of the form factors in HQS.

In order to compare our results with the available theoretical works [18,19,21] in heavy quark limit, we listed results from [18,19] in column 3 of Table 11. These analyses are mainly focused on CKM-favored decays. Note that the inconsistencies, in comparison, arise mainly due to the decay constants, mixing angle and their signs, and partially due to the difference of form-factors (owing to the different constituent quark masses) [18,19]. It has been pointed out, in CLF approach, result for $B(B^- \to \pi^- D_1^0)$ decay could only be explained if a positive sign is taken for $f_{D_1^{3/2}}$ decay constant, which conventionally should be negative (as taken in our results). It is worth mentioning that the CLF approach [19] also supports a large contribution from the color-suppressed amplitudes. Moreover, Jugeau et al. [21] and Cheng et al. [19] have used the experimental branching for $B^- \to \pi^- D_1^0$ decay to estimate the decay constants and form factors. It could be seen that the heavy quark corrections may result in the large deviations from the theoretical expectations in the present scenario.

Comparison with the LQCD inspired results

Now, we will focus on the results obtained by using the lattice QCD form factors, with a_1^{eff} and a_2^{eff} (40), which in turn yields the following branching ratios:

$$B(B^- \to \pi^- \underline{D}_1^0) = (0.9 \pm 0.1) \times 10^{-3}, \qquad B(B^- \to \pi^- D_1^0) = (5.7 \pm 2.0) \times 10^{-4}.$$

The calculated branching ratios for $B^- \to \pi^- \underline{D}_1^0$ and $B^- \to \pi^- D_1^0$ decays are in good agreement with the experimental observations. Here also, $B^- \to \pi^- \underline{D}_1^0$ receives dominant contribution from the color-favored transition and its branching ratio is roughly same as that of Class I $\bar{B}^0 \to \pi^- \underline{D}_1^+$ decay. The branching ratios of the color-favored decays are $B(\bar{B}^0 \to \pi^- \underline{D}_1^+) = (1.0 \pm 0.1) \times 10^{-3}$ and $B(\bar{B}^0 \to \pi^- D_1^+) = (1.3 \pm 0.3) \times 10^{-4}$.

We find that the lattice QCD inspired estimates are in good agreement with the experimental results and compare well with the other theoretical expectations [19,21,62]. It may be noted that the branching ratios in most of the theoretical works are calculated by ignoring the color-suppressed contributions under HQS. In this case, the branching ratios are compared with the assumption that D_1 is primarily $D_1^{1/2}$, while $\underline{D}_1$ is predominately $D_1^{3/2}$. For instance, the recent predictions based on the BT model gives $B(B^- \to \pi^- \underline{D}_1^0) = 1.25 \times 10^{-3}$ and $B(B^- \to \pi^- D_1^0) = 1.20 \times 10^{-4}$. Here also the discrepancy in comparison arise for $B(B^- \to \pi^- D_1^0)$ decay where color-suppressed contributions can play significant role. Jugeau et al. [21] has used a similar approach to extract the form factors $\tau_{1/2}(\omega)$ and $\tau_{3/2}(\omega)$ from the data and predicted the branching ratios for Class II decays: $B(\bar{B}^0 \to \pi^0 \underline{D}_1^0) = 2.2 \sim 2.8 \times 10^{-4}$ and $B(\bar{B}^0 \to \pi^0 D_1^0) < 3 \times 10^{-4}$. Concurrently, Jugeau et al. [21], has also been extracted $\tau_{1/2}(\omega)$ and $\tau_{3/2}(\omega)$ from the $B \to D^{**}\pi$ data by [19],

$$B^- \to \pi^- \underline{D}_1^0 \quad |\tau_{3/2}(1.32)| = 0.30 \pm 0.03$$
$$B^- \to \pi^- D_1^0 \quad |\tau_{1/2}(1.32)| < 0.19,$$

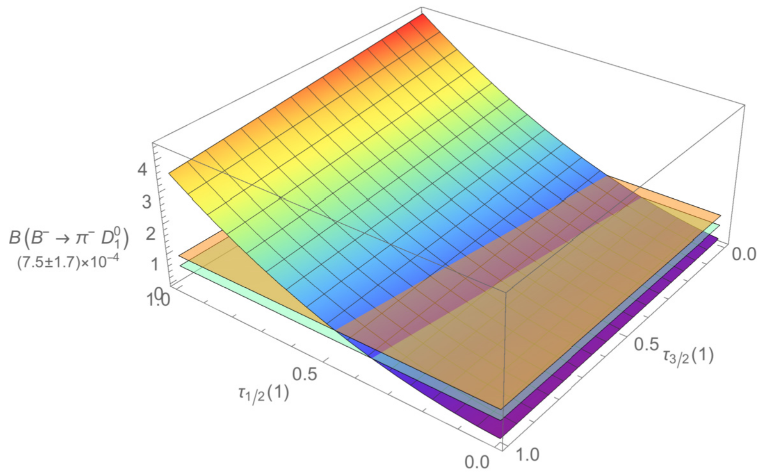

Fig. 4. The form factor dependence of the branching ratio of $B^- \to \pi^- D_1^0$ decay as a function of $\tau_{1/2}(1)$ and $\tau_{3/2}(1)$.

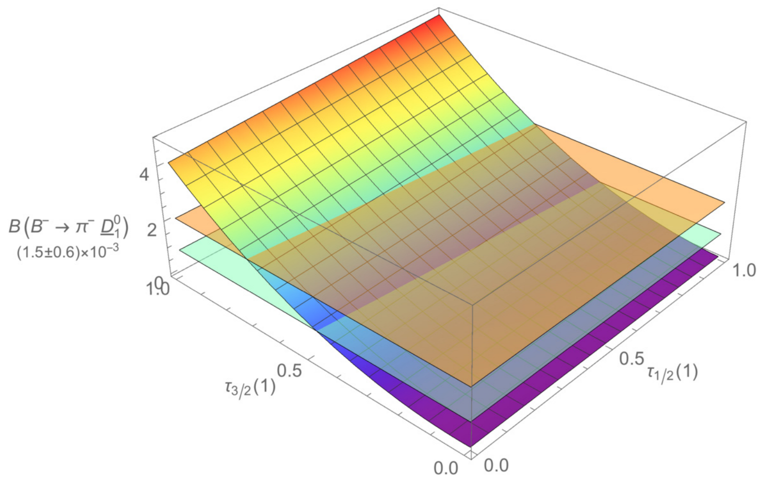

Fig. 5. The form factor dependence of the branching ratio of $B^- \to \pi^- \underline{D}_1^0$ decay as a function of $\tau_{1/2}(1)$ and $\tau_{3/2}(1)$.

which compares well with the present work,

$$|\tau_{3/2}(1.32)| = 0.34 \quad |\tau_{1/2}(1.32)| = 0.23.$$

A thorough review of the literature shows large range of the form factors, $\tau_{1/2}(1)$ and $\tau_{3/2}(1)$, at zero recoil ($\omega = 1$) based on the various theoretical approaches. Thus, it is reasonable to plot the branching ratio as a function of $\tau_{1/2}(1)$ and $\tau_{3/2}(1)$ to view the form factor dependence, as shown in Figs. 4 and 5. Different form factor values without any particular trend can give a reasonable guess on the type of uncertainties induced by the $1/m_Q$ corrections which could be pretty large. It can be argued that vanishing $B \to D^{**}$ transitions at zero recoil in the infinite mass limit, might give rise to non-vanishing results in the finite mass limit. This reflects the importance of the size of zero recoil contribution which may affect the branching ratios, significantly.

Table 12
HQS constrained branching ratios for $B \to PA$ decays in CKM-suppressed mode.

Decays	This Work	
	ISGW	LQCD
$\Delta b = 1, \Delta C = 1, \Delta S = -1$		
$B^- \to K^- D_1^0$	$(2.9 \pm 1.0) \times 10^{-5}$	$(4.0 \pm 1.2) \times 10^{-5}$
$B^- \to K^- \underline{D}_1^0$	$(1.8 \pm 0.2) \times 10^{-4}$	$(6.6 \pm 0.4) \times 10^{-5}$
$\bar{B}^0 \to \bar{K}^0 D_1^0$	$(9.6 \pm 3.8) \times 10^{-6}$	$(9.6 \pm 3.8) \times 10^{-6}$
$\bar{B}^0 \to \bar{K}^0 \underline{D}_1^0$	$(4.8 \pm 1.8) \times 10^{-7}$	$(4.8 \pm 1.8) \times 10^{-7}$
$\bar{B}^0 \to K^- D_1^+$	$(4.3 \pm 1.2) \times 10^{-6}$	$(0.9 \pm 0.2) \times 10^{-5}$
$\bar{B}^0 \to K^- \underline{D}_1^+$	$(1.9 \pm 0.3) \times 10^{-4}$	$(7.3 \pm 0.7) \times 10^{-5}$

One can also see that the relation (41) do hold true for color dominant decay modes *i.e.* $\bar{B} \to \pi \underline{D}_1$ due to $1/m_Q$ suppression of the color-suppressed contributions. However, it may be emphasized that the comparison with experimental results point towards the need of a deeper understanding of the color-suppressed contributions for $\bar{B} \to \pi D_1$ type decays. This indicates that the nonfactorizable contributions to color-suppressed transitions will be dominated by the nonperturbative effects.

On the other hand, in SCET, unlike naive a_2 factorization, the Class II decays are shown to be factorizable into a pion light-cone wave function and a $\bar{B} \to D^*$ soft distribution function [17,27]. Later, they have extended their formalism to the color-allowed and color-suppressed $\bar{B} \to D_1 M$ and $\bar{B} \to D_2^* M$ decays in the light of HQS constraints and give the relations for branching fractions in leading order (for equal strong phases in both channels):

$$\frac{B(\bar{B} \to D_2^* \pi)}{B(\bar{B} \to D_1 \pi)} = 1 \qquad (0.54 \pm 0.18)_{Expt}.$$

Clearly, this equality does not compete well with the existing experimental observation of 0.54 ± 0.18 by Belle [63]. Lastly, we list our results for CKM-favored and CKM-suppressed modes in the Table 11 and Table 12, respectively.

Estimates of nonfactorizable terms

In the scarcity of experimental data, the size of nonfactorizable contributions could be estimated from the recent model independent factorization assisted topological diagram analysis for $B \to D^* P$ decays [64]. S.H. Zhou et al. has used only four universal non-perturbative parameters, namely, χ^C, ϕ^C, χ^E, and ϕ^E to describe the contribution of the color-suppressed tree and W-exchange diagrams for all the $B \to D^* P$ decay channels in $b \to c$ transition. The amplitude expressions, in such case, can be given as [64],

$$\begin{aligned} T &= \sqrt{2} G_F V_{cb} V_{uq}^* a_1(\mu) f_V m_V F_1^{B\to P}(m_V^2)(\varepsilon_V^* \cdot p_B), \\ C &= \sqrt{2} G_F V_{cb} V_{uq}^* f_P m_V A_0^{B\to V}(m_V^2)(\varepsilon_V^* \cdot p_B) \chi^C e^{i\phi^C}, \\ E &= \sqrt{2} G_F V_{cb} V_{uq}^* m_V f_B \frac{f_P f_V}{f_D f_\pi} \chi^E e^{i\phi^E} (\varepsilon_V^* \cdot p_B), \end{aligned} \tag{43}$$

Table 13
Branching ratios for $B \to PA$ decays for nonfactorizable estimates.

Decays	Amplitude	Branching ratios		Expt.
		with phase	without phase	
$B^- \to \pi^- D_1^0$	$T+C$	$(6.85 \pm 0.80) \times 10^{-4}$	$(6.90 \pm 0.80) \times 10^{-4}$	$(7.5 \pm 1.7) \times 10^{-4}$
$B^- \to \pi^- \underline{D}_1^0$	$T+C$	$(1.8 \pm 0.4) \times 10^{-3}$	$(1.9 \pm 0.4) \times 10^{-3}$	$(1.5 \pm 0.6) \times 10^{-3}$
$B^- \to D^0 a_1^-$	$T+C$	$(1.0 \pm 0.1) \times 10^{-2}$	$(1.1 \pm 0.1) \times 10^{-2}$	$(4.0 \pm 4.0) \times 10^{-3}$
$\bar{B}^0 \to D^+ a_1^-$	$T+E$	$(8.0 \pm 0.8) \times 10^{-3}$	$(9.3 \pm 0.8) \times 10^{-3}$	$(6.0 \pm 3.3) \times 10^{-3}$

where, V denote vector meson. The T, C, and E represents the color-favored tree, color-suppressed tree and W-exchange diagram amplitudes, respectively (see for details [64]). The tree level amplitudes will depend mainly upon the choice of form factors, decay constants, and the parameters a_1 and a_2. The color-favored tree diagrams are evaluated from the factorization only, while color-suppressed tree and W-exchange diagrams involve universal parameters also. Their analysis yields the following numerical values for universal parameters χ^C, ϕ^C, χ^E, and ϕ^E for $B \to D^{(*)}P(V)$ [64],

$$\chi^C = 0.48 \pm 0.01, \quad \phi^C = (56.6^{+3.2}_{-3.8})^\circ, \quad \chi^E = 0.024^{+0.002}_{-0.001}, \quad \phi^E = (123.9^{+3.3}_{-2.2})^\circ. \tag{44}$$

Expecting that the analysis would also give reasonable estimate for the size of nonfactorizable terms in decays involving $D^{**}(\equiv D^*, D_1, D_1', D_2)$ mesons, we proceed in *scenario I* as follows. We obtain the expressions similar to (43) by replacing $V \to A$. Later, we calculate the branching ratios for experimentally known CKM-favored decays by using the universal coefficients of emission and exchange terms, with and without phases ($\phi^{C(E)}$), to include the nonfactorizable contributions in our analysis. Although, in order to have precise estimate in a model independent manner more experimental information is required. The results obtained in this scenario have been given in Table 13. We wish to point out that the branching ratios are smaller, in general, once the phases of the color-suppressed tree and W-exchange diagrams are included indicating the importance of nonfactorizable amplitudes as well as the signs of decay constants and QCD coefficients. For the decays obtaining contributions from the color-suppressed diagram, the amplitude decreases simply due to fact that the product $\chi^C\phi^C$ does not change sign and the magnitude of color-suppressed amplitude is reduced by a factor of $\chi^C\phi^C$. However, the contribution from the W-exchange amplitude interfere destructively with tree level contribution to give larger suppression in the branching ratio of $B \to D^+a_1^-$ decay. It is evident from the results that the nonfactorizable contribution though appear small, but have improved the agreement with respect to the experimental expectations.

Thus, the discrepancy between experimental and theoretical expectations in various formalism is evident. The resolution of all these issues require tremendous experimental and theoretical efforts in the near future.

6. Summary and conclusions

In this paper, we have studied the hadronic weak decays of bottom mesons emitting a pseudoscalar and an axial-vector mesons. We have employed the ISGW II [6] quark model to determine the $B \to A/A'$ transition form factors in, both, non-relativistic quark model framework as well as heavy quark symmetry constraints. Consequently, we obtained the branching ratios of $B \to PA$ decays in CKM-favored and CKM-suppressed modes. Firstly, we draw our observations in simple non-relativistic ISGW II framework as follows:

1. We apply the non-relativistic framework to determine the form factors and the branching ratios for $\bar{B} \to \pi D_1/Da_1$ decay modes. The branching ratios for these modes are of the order $10^{-2} \sim 10^{-4}$ which are in good agreement with the experimental results for $\theta_D = 17°$. It is interesting to note that the theoretical expectations favor the positive sign of mixing angle when compared with the experimental results.
2. Most of the branching ratios for the color-suppressed $\bar{B} \to \bar{K}_{(1)}\bar{D}_{(1)}$ type of decays are of the order $\mathcal{O}(10^{-4})$, which could be observed in near future. The CKM-suppressed, $\Delta b = 1, \Delta C = -1, \Delta S = -1$, mode also have few branching ratios in the range $10^{-4} \sim 10^{-6}$, which are well within the reach of current experiments.

In addition, we have analyzed the charm axial-vector meson emitting decays in ISGW II quark model and using the lattice QCD based form factors in *heavy quark symmetry constraints*. We obtained the branching ratios in CKM-favored modes and we list our findings as follows.

1. We have calculated the branching ratios for Class III type $\bar{B} \to \pi D_1$ decays. The $B(B^- \to \pi^- \underline{D}_1^0)$ and $B(B^- \to \pi^- D_1^0)$ decays in ISGW II framework are consistent with the experimental numbers within the error. Although, these decays get dominant contribution from the color-favored transition, still the color-suppressed contributions in $B^- \to \pi^- D_1^0$ decay can not be ignored. In heavy quark limit, the color-suppressed amplitudes are further suppressed by a factor of $1/m_Q$. Nonetheless, the experimental values require a larger contribution from the color-suppressed transitions. Therefore, the branching relations obtained in the heavy quark symmetry expectations: $B(B^- \to \pi^- \underline{D}_1^0) = B(\bar{B}^0 \to \pi^- \underline{D}_1^+)$ and $B(B^- \to \pi^- D_1^0) = B(\bar{B}^0 \to \pi^- D_1^+)$ may not be satisfied for the Class III type of decays. The experimental measurement of the ratio $B(B^- \to \pi^- D_1^0)/B(\bar{B}^0 \to \pi^- D_1^+)$ could provide a useful test for the heavy quark limit.
2. Furthermore, the analysis of $\bar{B} \to \pi D_1$ decay channels (in ISGW II) favors the choice of larger magnitude and negative sign for a_2^{eff}, which is further supported by comparison with the experimental observations. Moreover, the experimental data based on $B \to D\pi$ decays indicates the need of larger color-suppressed contributions. Thus, the large magnitude for the color-suppressed transition amplitude, a_2^{eff}, and a relatively smaller magnitude for the color-favored amplitude, a_1^{eff}, aid the experimental branching results for $B^- \to \pi^- D_1^0$ and $B^- \to \pi^- \underline{D}_1^0$ decay channels. It may also be pointed out that the smaller magnitude of color-favored Class I contributions bring our results closer to the other theoretical expectations.
3. In the lattice QCD inspired analysis, we find that the form factors extracted from the lattice QCD based $\tau_{1/2}(1)$ and $\tau_{3/2}(1)$ using the proper shape parameters match surprisingly well with the values extracted from the experimental data as well as some theoretical models. Hence, the obtained branching ratios match well with the experimental values. Here also, the analysis indicates relatively larger contribution from the color-suppressed transition amplitudes. At the same time, we wish to point out that the uncertainties in such phenomenological calculations could be large due to the expected $1/m_Q$ corrections.

Thus, the understanding of Class III decays which receive contributions from the constructive and destructive interferences of the color-favored and color-suppressed transitions, are of utmost importance to resolve the puzzle of larger magnitude of a_2. The theoretical uncertainties arising from the Λ_{QCD}/m_Q corrections to all the form factors in heavy quark expansion can be significant. Therefore, more precise experimental information on such decays will help the theory to assess the nonfactorizable contributions as well as the model independent phenomenological analyses of these processes.

Acknowledgement

One of the authors, R. Dhir, gratefully acknowledge the financial support by the Department of Science and Technology (CRG/2018/002796), New Delhi, India.

References

[1] J. Bjorken, Nucl. Phys. B, Proc. Suppl. 11 (1989) 325.
[2] M.J. Dugan, B. Grinstein, Phys. Lett. B 255 (1991) 583, and references therein.
[3] M. Bauer, B. Stech, M. Wirbel, Z. Phys. C 34 (1987) 103;
M. Wirbel, Prog. Part. Nucl. Phys. 21 (1988) 33, and references therein.
[4] M. Neubert, V. Rieckert, B. Stech, Q.P. Xu, in: A.J. Buras, M. Linder (Eds.), Heavy Flavors, World Scientific, Singapore, 1992;
S. Stone, Hadronic B decays, in: D.I. Britton, et al. (Eds.), 5th Int. Symp. on Heavy Flavor Physics, Editions Frontieres, Gif-sur-Yvette, 1993.
[5] N. Isgur, D. Scora, B. Grinstein, M.B. Wise, Phys. Rev. D 39 (1989) 799, and references therein.
[6] D. Scora, N. Isgur, Phys. Rev. D 52 (1995) 2783, and references therein.
[7] T.E. Browder, K. Honscheid, S. Playfer, B Decays, 2nd edn, ed., S. Stone World Scientific, Singapore, 1994.
[8] V.L. Chernyak, I.R. Zhitnitsky, Nucl. Phys. B 345 (1990) 137;
C.W. Bauer, et al., Phys. Rev. D 63 (2001) 114020, arXiv:hep-ph/0011336.
[9] H.Y. Cheng, C.K. Chua, Phys. Rev. D 69 (2004) 074025, and references therein.
[10] G. Claderon, et al., Phys. Rev. D 79 (2007) 094019, and references therein.
[11] H.Y. Cheng, K.C. Yang, Phys. Rev. D 76 (2007) 114020.
[12] H.Y. Cheng, K.C. Yang, Phys. Rev. D 78 (2008) 094001;
Erratum, Phys. Rev. D 79 (2009) 039903.
[13] K.C. Yang, Nucl. Phys. B, Proc. Suppl. 186 (2009) 399, and references therein.
[14] J.H. Munoz, N. Quintero, J. Phys. G 36 (2009) 125002.
[15] X. Liu, Z.J. Xiao, Phys. Rev. D 86 (2012) 074016;
X. Liu, et al., Phys. Rev. D 91 (2015) 014008;
X. Liu, et al., Phys. Rev. D 94 (2016) 113005, and references therein.
[16] A.C. Katoch, R.C. Verma, Int. J. Mod. Phys. 11 (1996) 129.
[17] S. Mantry, et al., Phys. Rev. D 68 (2003) 114009.
[18] H.Y. Cheng, Phys. Rev. D 67 (2003) 094007;
Phys. Rev. D 68 (2003) 094005.
[19] H.Y. Cheng, et al., Phys. Rev. D 74 (2006) 034020.
[20] A. Datta, et al., Phys. Lett. B 572 (2003) 164, arXiv:hep-ph/0307106.
[21] F. Jugeau, et al., Phys. Rev. D 72 (2005) 094010.
[22] C.H. Chen, Phys. Rev. D 68 (2003) 114008, arXiv:hep-ph/0310290.
[23] C.H. Chen, et al., Phys. Rev. D 69 (2004) 054002, arXiv:hep-ph/0307075.
[24] W.L. Ju, et al., J. High Energy Phys. 1509 (2015) 171.
[25] J. Segovia, et al., Phys. Rev. D 86 (2012) 014010.
[26] A. Faessler, et al., Phys. Rev. D 76 (2007) 014003.
[27] S. Mantry, Phys. Rev. D 70 (2004) 114006.
[28] F. Jugeau, A. Le Yaouanc, L. Oliver, J.-C. Raynal, Phys. Rev. D 72 (2005) 094010, arXiv:hep-ph/0504206.
[29] A. Le Yaouanc, O. Pène, Int. J. Mod. Phys. A 30 (2015) 1543009, arXiv:1408.5104 [hep-ph].
[30] A. Le Yaouanc, L. Oliver, J.-C. Raynal, H.-R. Dong, Phys. Rev. D 90 (2014) 114014, arXiv:1407.1152 [hep-ph].
[31] D. Becirevic, A. Le Yaouanc, L. Oliver, J.C. Raynal, P. Roudeau, J. Serrano, Phys. Rev. D 87 (2013) 054007, arXiv:1206.5869 [hep-ph].

[32] D. Bečirević, A. Le Yaouanc, L. Oliver, J.C. Raynal, Phys. Rev. D 96 (2017) 036018, arXiv:1705.05667 [hep-ph].
[33] V. Morenas, A. Le Yaouanc, L. Oliver, O. Pene, J.C. Raynal, Phys. Lett. B 408 (1997) 357, arXiv:hep-ph/9705324.
[34] D. Becirevic, B. Blossier, P. Boucaud, G. Herdoiza, J.P. Leroy, A. Le Yaouanc, V. Morenas, O. Pene, Phys. Lett. B 609 (2005) 298, arXiv:hep-lat/0406031.
[35] B. Blossier, et al., European Twisted Mass Collaboration, J. High Energy Phys. 0906 (2009) 022, arXiv:0903.2298 [hep-lat].
[36] M. Atoui, arXiv:1305.0462 [hep-lat].
[37] M. Atoui, B. Blossier, V. Morénas, O. Pène, K. Petrov, Eur. Phys. J. C 75 (2015) 376, arXiv:1312.2914 [hep-lat].
[38] R.C. Verma, J. Phys. G 39 (2012) 025005.
[39] F.U. Bernlochner, Z. Ligeti, Phys. Rev. D 95 (2017) 014022, arXiv:1606.09300 [hep-ph].
[40] H.X. Chen, et al., Rep. Prog. Phys. 80 (2017) 076201.
[41] Patrignani, et al., Particle Data Group, Chin. Phys. C 40 (2016) 100001.
[42] A. Al-Haydari, et al., QCDSF Collaboration, Eur. Phys. J. A 43 (2010) 107, arXiv:0903.1664 [hep-lat].
[43] H. Na, et al., HPQCD Collaboration, Phys. Rev. D 92 (2015) 054510, Erratum: Phys. Rev. D 93 (2016) 119906, arXiv:1505.03925 [hep-lat].
[44] J. Dingfelder, T. Mannel, Rev. Mod. Phys. 88 (2016) 035008.
[45] G. Duplancic, B. Melic, J. High Energy Phys. 1511 (2015) 138, arXiv:1508.05287 [hep-ph].
[46] H.Y. Cheng, Phys. Lett. B 707 (2012) 116.
[47] N. Isgur, M.B. Wise, Phys. Rev. D 43 (1991) 819.
[48] K. Abe, et al., Belle Collaboration, Phys. Rev. D 69 (2004) 112002.
[49] P. Colangelo, et al., Phys. Lett. B 634 (2006) 235.
[50] M. Beneke, G. Buchalla, M. Neubert, C.T. Sachrajda, Nucl. Phys. B 591 (2000) 313, arXiv:hep-ph/0006124, and references therein.
[51] M. Neubert, B. Stech, Adv. Ser. Dir. High Energy Phys. 15 (1998) 294, arXiv:hep-ph/9705292.
[52] M. Neubert, A.A. Petrov, Phys. Lett. B 519 (2001) 50, https://doi.org/10.1016/S0370-2693(01)01093-0, arXiv:hep-ph/0108103.
[53] H.Y. Cheng, Phys. Rev. D 65 (2002) 094012, and references therein.
[54] H.Y. Cheng, Flavor Physics, ICFP2001, 2002, arXiv:hep-ph/0109259.
[55] G.L. Wang, Phys. Lett. B 650 (2007) 15.
[56] M. Suzuki, Phys. Rev. D 47 (1993) 1252.
[57] M. Suzuki, Phys. Rev. D 55 (1997) 2840.
[58] J.C.R. Bloch, et al., Phys. Rev. D 59 (1999) 111502.
[59] V. Morenas, A. Le Yaouanc, L. Oliver, O. Pene, J.C. Raynal, Phys. Lett. B 408 (1997) 357, arXiv:hep-ph/9705324.
[60] N. Uraltsev, Phys. Lett. B 501 (2001) 86.
[61] J.D. Bjorken, SLAC-PUB-5278, 1990;
J.D. Bjorken, J. Dunietz, J. Taron, Nucl. Phys. B 371 (1992) 111.
[62] I.I. Bigi, B. Blossier, A. Le Yaouanc, L. Oliver, O. Pene, J.-C. Raynal, A. Oyanguren, P. Roudeau, Eur. Phys. J. C 52 (2007) 975, arXiv:0708.1621 [hep-ph].
[63] K. Abe, et al., Belle Collaboration, Phys. Rev. Lett. 94 (2005) 221805.
[64] S.H. Zhou, Y.B. Wei, Q. Qin, Y. Li, F.S. Yu, C.D. Lu, Phys. Rev. D 92 (2015) 094016, https://doi.org/10.1103/PhysRevD.92.094016, arXiv:1509.04060 [hep-ph], and references therein.